BE 159: Signal Transduction and Mechanics in Morphogenesis

Justin Bois

Caltech

Winter, 2020

This document was prepared at Caltech with financial support from the Donna and Benjamin M. Rosen Bioengineering Center.

1 Welcome

The first lecture provided a course overview. It is not really conducive for written notes. The slides may be downloaded here.

2 Biochemical kinetics in signaling

When we look at a picture of how signaling works in a cell, as in Fig. 1, we see that a variety of processes occur along the signaling pathway. There is ligand binding to receptors that are embedded in a two-dimensional surface, the cell membrane. There is the transport, either passive by diffusion or active by motor proteins, of signaling molecules or transcription factors through the cytoplasm. Then, the transcription factor needs to get into the nucleus via nuclear pore complexes. From there, it needs to find the appropriate promoter to bind on the genome, an interesting transport problem by itself. There are plenty of interactions with the machinery involved in transcription, post transcriptional modifications, and eventual export from the nucleus. There are lots and lots of kinetic processes! We might throw our hands up in the air and scream that we do not know how to model *all* of that.

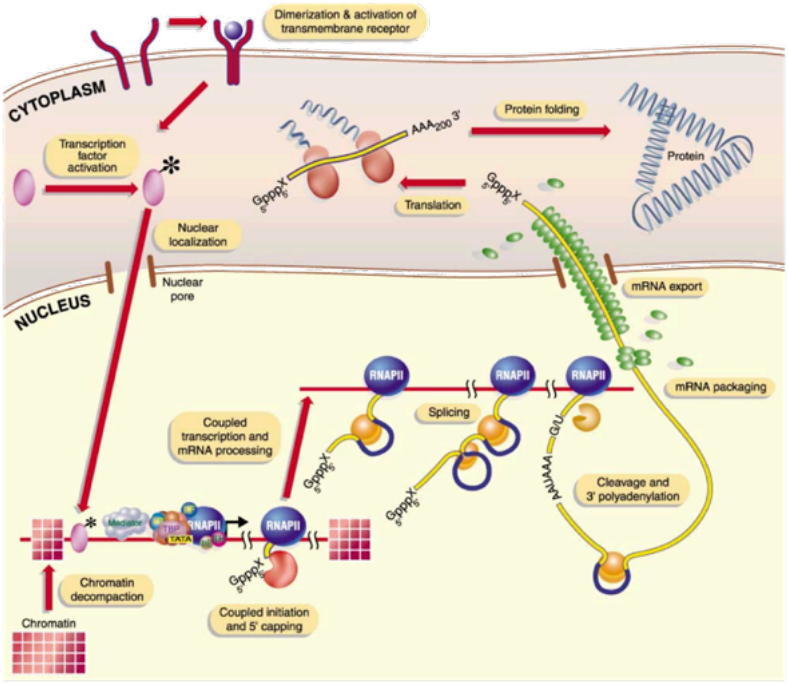

Figure 1: Schematic of a generic signaling pathway. Taken from Orphanides and Reinberg, *Cell*, **108**, 429–451, 2002.

So how do we overcome this modeling paralysis and proceed to develop physical description of these processes? There are a few main ideas we can consider to deal with this issue.

1. **Separation of time scales.** Some of the processes that happen along a signaling pathway are very fast compared to others. So, if we are interested in the dynamics of the entire pathway, say in terms of the more global response of a

cell to a variation in ligand concentration, we can ignore the fast processes, or at least assume that fast dynamics reach equilibrium rapidly.

2. **Assumption of Poisson processes.** In this context, a Poisson process may be thought of as a series of well-defined, separate events that occur randomly, without memory of what has occurred before. This is often the case for things like molecular collisions. If we model the events along a signaling pathway as Poisson processes, we can at least write down equations to describe the dynamics.

3. **Consideration only of average properties.** Instead of keeping track of what each molecule in the cell is doing, we can instead only consider how the *concentrations* of molecular species.

In what follows, we will put these approximations to use to arrive a **mass action kinetics** to describe the dynamics of molecules involved in cell signaling, and indeed in many other cellular processes. These ideas are central to the Goentoro and Kirschner paper, and will come into play throughout the rest of the course.

2.1 Thinking probabilistically: Master equations

Let us define very broadly a state s of a system to include all molecular species. Whenever there is a change of state, say from s' to s, there is a unit change in molecular species. For example, two proteins molecules that are bound to each other can separate, and this would lead to a state change. You can imagine that the state space available to all molecules in a cell is enormous. Nonetheless, let us move forward to write down a **master equation** to describe the dynamics of the *probability* that the molecular species of a cell are in state s at time t, which we denote as $P(s,t)$.

Generally, a master equation is a loss-gain equation for probabilities of states governed by a Markov process.[1] Specifically,

$$\frac{\mathrm{d}P(s,t)}{\mathrm{d}t} = \sum_{s'} \left[W(s \mid s')P(s',t) - W(s' \mid s)P(s,t) \right]. \tag{2.1}$$

Here, $W(s \mid s')$ is the transition probability per unit time of going from s' to s. Note that there is an ODE for *each* of the many many many states s.

The master equation makes sense by inspection and appears simple. The nuance lies in the definition of the transition rates, $W(s \mid s')$. There is also the computational difficulty that state space is enormous. In general, solving the master equation is difficult and is usually intractable analytically.

[1] A good reference for studying master equations is *Stochastic Processes in Physics and Chemistry* by N. G. van Kampen.

To make some more progress, let's restrict what we call a "state." We will define a state to be a set of copy numbers of molecular species. At this point, it helps to be less abstract and think of a concrete example. Consider the case where two signaling molecules, a and b may bind and unbind to each other, and these are the only molecules we are considering. There are then three molecular species a, b, and ab. We then define a state by the copy numbers of these respective species.

$$s \to \mathbf{n} \equiv (n_{\mathrm{a}}, n_{\mathrm{b}}, n_{\mathrm{ab}}). \tag{2.2}$$

Then, we can re-write the master equation as

$$\frac{\mathrm{d}P(\mathbf{n},t)}{\mathrm{d}t} = \sum_{\mathbf{n}'} \left[W(\mathbf{n} \mid \mathbf{n}')P(\mathbf{n}',t) - W(\mathbf{n}' \mid \mathbf{n})P(\mathbf{n},t) \right]. \tag{2.3}$$

2.2 Assigning the transition rates

Since the events that change the state are binding of an a and a b molecule or the dissociation of an ab complex, we know that very many of the transition rates, $W(\mathbf{n} \mid \mathbf{n}')$ are zero. Specifically, $W(n_{\mathrm{a}}, n_{\mathrm{b}}, n_{\mathrm{ab}} \mid n'_{\mathrm{a}}, n'_{\mathrm{b}}, n'_{\mathrm{ab}}) = 0$ for all cases except:

$$\begin{aligned} n_{\mathrm{ab}} &= n'_{\mathrm{ab}} - 1,\ n_{\mathrm{a}} = n'_{\mathrm{a}} + 1,\ n_{\mathrm{b}} = n'_{\mathrm{b}} + 1 \quad \text{(dissociation)} \\ \text{or } n_{\mathrm{ab}} &= n'_{\mathrm{ab}} + 1,\ n_{\mathrm{a}} = n'_{\mathrm{a}} - 1,\ n_{\mathrm{b}} = n'_{\mathrm{b}} - 1 \quad \text{(binding).} \end{aligned} \tag{2.4}$$

What value should we assign $W(\mathbf{n} \mid \mathbf{n}')$ for these two cases? Consider first dissociation. The probability per unit time of getting a dissociation event should be dependent on the number of ab complexes there are. If there are no ab complexes, the probability of getting a dissociation is zero. If we further assume that the complexes are all independent of each other, valid in the *dilute limit*, then the probability of observing a transition should be proportional to the number of ab complexes. Finally, since we model all processes as Poisson processes, there is no memory, so therefore no temporal dependence. So, we have

$$W_{\mathrm{dissoc}} = k_{-1}\, n_{\mathrm{ab}}, \tag{2.5}$$

where k_{-1} is a constant. (The subscript -1 denotes dissociation; we will use the subscript 1 for binding.)

Now, let's consider binding. Again, the transition rate for binding should be independent of time because we are dealing with Poisson processes. In order for a binding event to happen, two molecules need to collide. The probability of collision should scale with the copy number of each species, a and b. It should also scale inversely with the available volume (or surface area if we are talking about binding

events on a membrane). In other words the bigger the volume, the less likely it is to observe a collision.[2] So, we have

$$W_{\text{binding}} = k_1 n_{\text{a}} n_{\text{b}} / V, \tag{2.6}$$

where V is the volume of the cell or system of interest.

Now that we know our transition rates, we can rewrite the master equation.

$$\begin{aligned}\frac{\mathrm{d}P(n_{\text{a}}, n_{\text{b}}, n_{\text{ab}}, t)}{\mathrm{d}t} = &\frac{k_1}{V}(n_{\text{a}}+1)(n_{\text{b}}+1)P(n_{\text{a}}+1, n_{\text{b}}+1, n_{\text{ab}}-1, t) \\ &+ k_{-1}(n_{\text{ab}}+1)P(n_{\text{a}}-1, n_{\text{b}}-1, n_{\text{ab}}+1, t) \\ &- \left(\frac{k_1}{V} n_{\text{a}} n_{\text{b}} + k_{-1} n_{\text{ab}}\right) P(n_{\text{a}}, n_{\text{b}}, n_{\text{ab}}, t),\end{aligned} \tag{2.7}$$

where it is understood that $P(n_{\text{a}}, n_{\text{b}}, n_{\text{ab}}, t)$ is zero if any of n_{a}, n_{b}, or n_{ab} are less than zero.

2.3 Dynamics of averages

We now have a workable master equation, but there still many, many equations. If we instead consider instead how the *average* number of each species changes over time, we can greatly reduce the number of equations. In doing this, we are throwing out much of the information contained in the probability distribution $P(\mathbf{n}, t)$, considering only its first moment. With that caveat in mind, let's compute the first moment. Recall that the average number of a molecules is

$$\langle n_{\text{a}} \rangle (t) = \sum_{n_{\text{a}}=0}^{\infty} n_{\text{a}} \, P(n_{\text{a}}, t), \tag{2.8}$$

with

$$P(n_{\text{a}}, t) = \sum_{n_{\text{b}}=0}^{\infty} \sum_{n_{\text{ab}}=0}^{\infty} P(n_{\text{a}}, n_{\text{b}}, n_{\text{ab}}, t), \tag{2.9}$$

thereby giving

$$\langle n_{\text{a}} \rangle (t) = \sum_{n_{\text{a}}=0}^{\infty} \sum_{n_{\text{b}}=0}^{\infty} \sum_{n_{\text{ab}}=0}^{\infty} n_{\text{a}} \, P(n_{\text{a}}, n_{\text{b}}, n_{\text{ab}}, t). \tag{2.10}$$

[2] That the transition rate is proportional to V^{-1} and not, say, V^{-2} requires some careful analysis we will not go into here.

So, we will multiply both sides of equation (2.7) by n_a and apply the triple sum

$$\sum_{n_\mathrm{a}=0}^{\infty}\sum_{n_\mathrm{b}=0}^{\infty}\sum_{n_\mathrm{ab}=0}^{\infty} \tag{2.11}$$

to the resulting equation. Evaluation of the left hand side of equation (2.7) is trivial.

$$\sum_{n_\mathrm{a}=0}^{\infty}\sum_{n_\mathrm{b}=0}^{\infty}\sum_{n_\mathrm{ab}=0}^{\infty} n_\mathrm{a}\,\frac{\mathrm{d}P(n_\mathrm{a},n_\mathrm{b},n_\mathrm{ab},t)}{\mathrm{d}t} = \frac{\mathrm{d}\langle n_\mathrm{a}\rangle}{\mathrm{d}t}. \tag{2.12}$$

The last two terms on the right hand side are the easiest to evaluate.

$$\begin{aligned}-\sum_{n_\mathrm{a}=0}^{\infty}\sum_{n_\mathrm{b}=0}^{\infty}\sum_{n_\mathrm{ab}=0}^{\infty}\frac{k_1}{V}\,n_\mathrm{a}^2 n_\mathrm{b}\,P(n_\mathrm{a},n_\mathrm{b},n_\mathrm{ab},t) &= -\frac{k_1}{V}\sum_{n_\mathrm{a}=0}^{\infty}\sum_{n_\mathrm{b}=0}^{\infty} n_\mathrm{a}^2 n_\mathrm{b}\,P(n_\mathrm{a},n_\mathrm{b},t)\\ &= -\frac{k_1}{V}\,\langle n_\mathrm{a}^2 n_\mathrm{b}\rangle. \end{aligned} \tag{2.13}$$

Similarly,

$$-\sum_{n_\mathrm{a}=0}^{\infty}\sum_{n_\mathrm{b}=0}^{\infty}\sum_{n_\mathrm{ab}=0}^{\infty} k_{-1} n_\mathrm{a} n_\mathrm{ab}\,P(n_\mathrm{a},n_\mathrm{b},n_\mathrm{ab},t) = -k_{-1}\langle n_\mathrm{a} n_\mathrm{ab}\rangle. \tag{2.14}$$

In these expressions, for notational convenience, we have not written the explicit time dependence of the averages. Now, we will work on the first sum on the right hand side.

$$\begin{aligned}&\sum_{n_\mathrm{a}=0}^{\infty}\sum_{n_\mathrm{b}=0}^{\infty}\sum_{n_\mathrm{ab}=0}^{\infty}\frac{k_1}{V}\,n_\mathrm{a}(n_\mathrm{a}+1)(n_\mathrm{b}+1)P(n_\mathrm{a}+1,n_\mathrm{b}+1,n_\mathrm{ab}-1,t)\\ &\quad= \frac{k_1}{V}\sum_{n_\mathrm{a}=0}^{\infty}\sum_{n_\mathrm{b}=0}^{\infty}\sum_{n_\mathrm{ab}=0}^{\infty} n_\mathrm{a}(n_\mathrm{a}+1)(n_\mathrm{b}+1)P(n_\mathrm{a}+1,n_\mathrm{b}+1,n_\mathrm{ab},t)\\ &\quad= \frac{k_1}{V}\sum_{n_\mathrm{a}=0}^{\infty}\sum_{n_\mathrm{b}=0}^{\infty} n_\mathrm{a}(n_\mathrm{a}+1)(n_\mathrm{b}+1)P(n_\mathrm{a}+1,n_\mathrm{b}+1,t)\\ &\quad= \frac{k_1}{V}\sum_{n_\mathrm{a}=0}^{\infty}\sum_{n_\mathrm{b}=0}^{\infty}(n_\mathrm{a}-1)n_\mathrm{a} n_\mathrm{b}\,P(n_\mathrm{a},n_\mathrm{b},t)\\ &\quad= \frac{k_1}{V}\left(\langle n_\mathrm{a}^2 n_\mathrm{b}\rangle - \langle n_\mathrm{a} n_\mathrm{b}\rangle\right). \end{aligned} \tag{2.15}$$

And finally, the second sum on the right hand side.

$$\sum_{n_\mathrm{a}=0}^{\infty}\sum_{n_\mathrm{b}=0}^{\infty}\sum_{n_\mathrm{ab}=0}^{\infty} k_{-1} n_\mathrm{a}(n_\mathrm{ab}+1)P(n_\mathrm{a}-1,n_\mathrm{b}-1,n_\mathrm{ab}+1,t)$$

$$= k_{-1} \sum_{n_a=0}^{\infty} \sum_{n_b=0}^{\infty} \sum_{n_{ab}=0}^{\infty} n_a(n_{ab}+1)P(n_a-1, n_b, n_{ab}+1, t)$$

$$= k_{-1} \sum_{n_a=0}^{\infty} \sum_{n_{ab}=0}^{\infty} n_a(n_{ab}+1)P(n_a-1, n_{ab}+1, t)$$

$$= k_{-1} \sum_{n_a=0}^{\infty} \sum_{n_{ab}=0}^{\infty} (n_a+1)n_{ab}P(n_a, n_{ab}, t)$$

$$= k_{-1} \left(\langle n_a n_{ab} \rangle + \langle n_{ab} \rangle \right). \tag{2.16}$$

Now that we have computed all of the sums, let's put it all together.

$$\frac{\mathrm{d}\langle n_a \rangle}{\mathrm{d}t} = \frac{k_1}{V} \left(\langle n_a^2 n_b \rangle - \langle n_a n_b \rangle \right) + k_{-1} \left(\langle n_a n_{ab} \rangle + \langle n_{ab} \rangle \right) - \frac{k_1}{V} \langle n_a^2 n_b \rangle - k_{-1} \langle n_a n_{ab} \rangle$$

$$= -k_1 \frac{\langle n_a n_b \rangle}{V} + k_{-1} \langle n_{ab} \rangle. \tag{2.17}$$

If we assume that the particle counts of species a and species b are independent, then $\langle n_a n_b \rangle = \langle n_a \rangle \langle n_b \rangle$. Then, we have

$$\frac{\mathrm{d}\langle n_a \rangle}{\mathrm{d}t} = -k_1 \frac{\langle n_a \rangle \langle n_b \rangle}{V} + k_{-1} \langle n_{ab} \rangle. \tag{2.18}$$

The thermodynamic *concentration* of species i is $c_i = \langle n_i \rangle / V$. So, if we divide both sides of the above equation by V, we get

$$\frac{\mathrm{d}c_a}{\mathrm{d}t} = -k_1 c_a c_b + k_{-1} c_{ab}. \tag{2.19}$$

If we do the same averaging technique with n_b and n_{ab}, we get

$$\frac{\mathrm{d}c_b}{\mathrm{d}t} = -k_1 c_a c_b + k_{-1} c_{ab}, \tag{2.20}$$

$$\frac{\mathrm{d}c_{ab}}{\mathrm{d}t} = k_1 c_a c_b - k_{-1} c_{ab}. \tag{2.21}$$

We now have three equations in terms of concentrations that we derived from the master equation.

2.4 The law of mass action

Chemical rate equations like those we just derived, in which the rate of a chemical reaction is proportional to the products of the concentrations of the participating

molecular species follow the **law of mass action**, often referred to as **mass action kinetics**.

It is important to recall all of the assumptions we made to get here.

1. Events that change state are Poisson processes. Implicit in this assumption is that the binding or dissociation (or any other event) happens essentially instantaneously with well-defined pauses between them. This is one instance of where a separation of time scales is important.
2. All molecular species are independent of each other; i.e., we are in the dilute limit.
3. In our last step, by taking $\langle n_\mathrm{a} n_\mathrm{b} \rangle \approx \langle n_\mathrm{a} \rangle \langle n_\mathrm{b} \rangle$, we tacitly assumed that $P(n_\mathrm{a}, n_\mathrm{b}, t) \approx P(n_\mathrm{a}, t) P(n_\mathrm{b}, t)$, i.e., that n_a and n_b are independent of each other, or that they have small covariance. Note that this is not always necessarily the case, especially at small copy number.

In addition to these assumptions, we are willfully throwing out all information about the probability distributions of the states we're modeling, except for the first moment (the mean).

Going forward in the course, we will use and abuse the law of mass action extensively. Especially when the copy number of molecules are small, this could lead to trouble. We might miss the important of noise (since we are neglecting fluctuations), or some of the underlying assumptions might not be valid. Nonetheless, the law of mass action is one of those approximate theories that is "unreasonably effective" in the sense that we are surprised at how well it tends to work in matching experimental observation.

2.5 Sigmoidal rate dependence?

If you have studied systems biology, you often find expressions for rates that are sigmoidal in shape, such as

$$\frac{\mathrm{d}c}{\mathrm{d}t} = \frac{k_1}{k_2 + c^2}, \tag{2.22}$$

a famous Hill function. This does not look like mass action at face. Where does this come from?

You may be familiar with Michaelis-Menten kinetics for enzymatic activity. In this scheme, a substrate s reacts with an enzyme e to form an intermediate which then forms a product p according to the mechanism

$$e + s \underset{k_{-1}}{\overset{k_1}{\rightleftharpoons}} se \xrightarrow{q_1} e + p. \tag{2.23}$$

Now, let's consider the case where the complex se might bind another substrate in the reaction

$$se + s \underset{k_{-2}}{\overset{k_2}{\rightleftharpoons}} s_2e \xrightarrow{q_2} se + p. \tag{2.24}$$

There are now six reactions in total and a total of five species. We could write master equations, perform averages, and then get the mass action expressions, but we will just directly write the mass action ODEs directly.

$$\frac{\mathrm{d}c_s}{\mathrm{d}t} = -k_1 c_e c_s + k_{-1} c_{se} - k_2 c_{se} c_s + k_{-2} c_{s_2e}, \tag{2.25}$$

$$\frac{\mathrm{d}c_e}{\mathrm{d}t} = -k_1 c_e c_s + (k_{-1} + q_1) c_{se}, \tag{2.26}$$

$$\frac{\mathrm{d}c_{se}}{\mathrm{d}t} = k_1 c_e c_s - (k_{-1} + q_1) c_{se} - k_2 c_{se} c_s + (k_{-2} + q_2) c_{s_2e}, \tag{2.27}$$

$$\frac{\mathrm{d}c_{s_2e}}{\mathrm{d}t} = k_2 c_{se} c_s - (k_{-2} + q_2) c_{s_2e}, \tag{2.28}$$

$$\frac{\mathrm{d}c_p}{\mathrm{d}t} = q_1 c_{se} + q_2 c_{s_2e}. \tag{2.29}$$

We are primarily interested in the rate of consumption of substrate, so we seek a simple expression for $\dot{c}_s$ in terms of the total enzyme and substrate concentration. Toward this end, we make a **pseudo steady state approximation** that $\dot{c}_{se} - \dot{c}_{s_2e} = 0$. This means that the concentrations of the intermediates do not change appreciably on the time scale of product formation. Again, this is an instance where separation of time scales allows us to make useful approximations to simplify the mathematics. As a result, we have

$$k_1 c_e c_s = (k_{-1} + q_1) c_{se}, \tag{2.30}$$

$$k_2 c_{se} c_s = (k_{-2} + q_2) c_{s_2e}. \tag{2.31}$$

We can rewrite the first of these equation as

$$c_e c_s = K_{M,1} c_{se}, \tag{2.32}$$

where

$$K_{M,1} \equiv \frac{k_{-1} + q_1}{k_1} \tag{2.33}$$

is the Michaelis constant for the first reaction. We also get

$$c_e c_s^2 = K_{M,1} K_{M,2} c_{s_2e}, \tag{2.34}$$

with

$$K_{M,2} \equiv \frac{k_{-2} + q_2}{k_2}. \tag{2.35}$$

Since the total amount of enzyme is conserved, we define the constant amount of enzyme

$$c_e^{\text{tot}} \equiv c_e + c_{se} + c_{s_2e}. \tag{2.36}$$

Using this relation along with equations (2.34) and (2.36) allows us to write an expression for c_e in terms of c_e^{tot} and c_s.

$$c_e = c_e^{\text{tot}} \left(1 + \frac{c_s}{K_{M,1}} + \frac{c_s^2}{K_{M,1}K_{M,2}}\right)^{-1}. \tag{2.37}$$

Substituting this expression, along with equations (2.34) and (2.36) into the expression for $\dot{c}_s$ (equation (2.25)) gives, after simplification

$$\frac{\mathrm{d}c_s}{\mathrm{d}t} = -\frac{c_e^{\text{tot}}\left(q_1 K_{M,2} c_s + q_2 c_s^2\right)}{K_{M,1}K_{M,2} + K_{M,2}c_s + c_s^2}. \tag{2.38}$$

This equation has a sigmoidal form, and it looks like a typical phenomenological Hill function (2.22) in certain limits. In particular, if $q_1 \approx 0$, that is if only the doubly-complexed substrate can produce product, the numerator becomes $q_2 c_e^{\text{tot}} c_s^2$. Further, if $K_{M,2} \ll c_s \ll K_{M,1}$, the denominator becomes $K_{M,1}K_{M,2} + c_s^2$. This means that once one substrate molecules is bound to an enzyme, the second binds much faster (its Michaelis constant is smaller). These limits are hallmarks of cooperativity. The result is

$$\frac{\mathrm{d}c_s}{\mathrm{d}t} = -\frac{q_2 c_e^{\text{tot}} c_s^2}{K_{M,1}K_{M,2} + c_s^2}. \tag{2.39}$$

which has the same form as the Hill equation (2.22) with Hill coefficient of 2.

The important lesson here is that many molecular mechanisms can give kinetics that relate to phenomenological Hill equations. But the Hill equation by itself says very little about the underlying mechanism. In my view, if you have a molecular mechanism in mind, it is best to derive the actual expressions you want to use. In fact, because it is not difficult to numerically solve a system of ODEs, you are often better off just directly solving the original mass action ODEs you write down without approximation. In the Goentoro and Kirschner paper, however, you will see that the big advantage of carefully doing analytical work, nondimensionalizing, and making reasonable approximations is that you can draw more general conclusions and sometimes expose structure to the system that might otherwise be difficult to see.

2.6 Sigmoidal rates of gene expression

If we are interested in the kinetics of actual gene products, not just intermediates along the signaling pathway, we need to model the gene expression levels. This is often down by throwing Hill functions around. However, I encourage you to not do this, but rather to think carefully about the structure of the promoter region and the transcription factors that bind it. If you take BE/APh 161, this will be covered in detail, and I omit it in this course.

3 Wnt signaling

In this lecture, we will discuss methods for modeling biochemical networks using mass action kinetics with the example of **Wnt signaling** as our motivation.

3.1 Introduction to Wnt signaling

The Wnt (pronounced "wint") signaling pathway is central in many developmental processes. To see how central it is, you might want to visit the Wnt homepage, run by Roel Nusse's lab at Stanford, which details the components of the pathway as well as a wealth of links to other information.

The history of the discovery of the Wnt family of proteins highlights its importance in development. In their Nobel Prize-winning work published in 1980, Nüsslein-Volhard and Wieschaus discovered several genes that are central to development in *Drosophila*. One of these was a segment polarity gene Wingless (Wg). The gene was so named because of its phenotype: wingless adult flies, so the gene has downstream effects past regulation of segment polarity. A couple years later, Nusse and Varmus discovered a gene in mice where mutations caused breast cancer, which they named integration 1, or int1. It was later discovered that int1 is highly conserved across species, including *Drosophila*, and that it was part of the same family as Wg. Going forward, this family of genes was referred to as Wnt, a combination of Wg and int.

During development, as we have mentioned in class, neighboring cells need to communicate to each other for differentiation. Beyond that, they need to sense their environment; e.g., they need to make changes to gene expression levels depending on external morphogen concentrations. In order to accomplish this, the "signal" must cross the cell membrane.

The Wnt pathway, shown in Fig. 2 is one major signaling pathway for accomplishing this. The transmembrane proteins Frizzled and LRP (lipoprotein receptor-related protein) are Wnt's binding partners. When unbound to Wnt, these proteins do not interfere with the destruction cycle of β-catenin, an important transcription factor (more on β-catenin soon). At the center of this destruction cycle is a complex of axin and adenomatous polyposis coli (APC), the latter so named because in humans it was found to be a colorectal tumor suppressor. This complex is commonly referred to as the axin complex. It recuits casein kinase 1 (CK1) and glycogen synthase kinase 3 (GSK-3), which phosphorylate β-catenin. The phosphorylated β-catenin is then targeted by β-TrCP, which promotes polyubiquitinization of the phosphorylated β-catenin, which is then degraded by the proteasome.

When Wnt is present outside of the cell membrane, it binds to Fizzled and LRP,

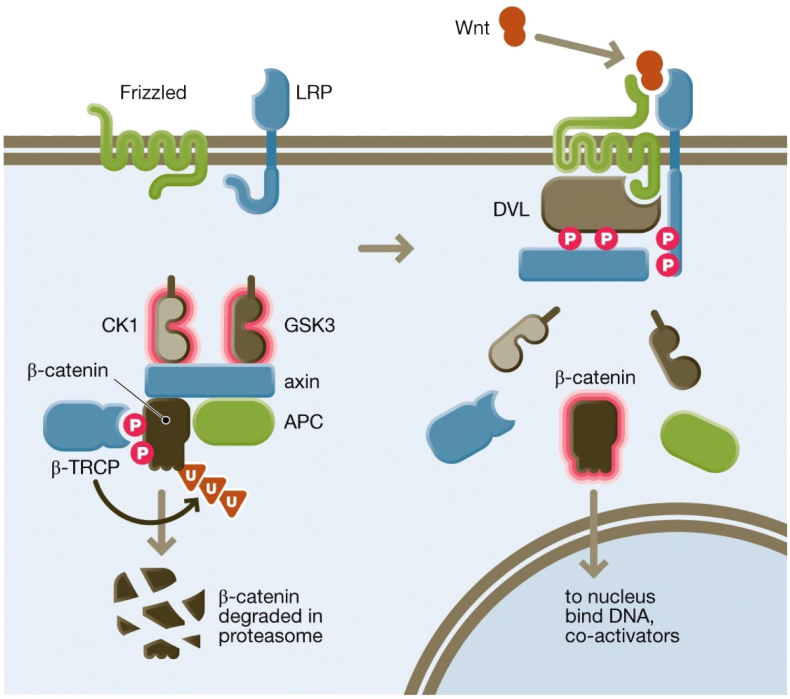

Figure 2: Schematic of the Wnt signaling pathway. Taken from Fig. 8.15 of Lim, Mayer, and Pawson, *Cell Signaling*, Garland Science, 2015.

bringing them together as a heterodimer. In this configuration, Frizzled mediates the phosphorlyation and activation of Dishevelled (DVL, a.k.a. Dsh), which then has a strong affinity for axin. Furthermore, the tail of LRP is available for phosphorylation by CK1 and GSK-3. Thus, this activated Frizzled/LRP complex attracts the components of the degradation complex, thereby making them less available for degrading β-catenin. As a result, stable, unphosphorylated β-catenin can enter the nucleus. It then binds its coactivators, e.g., the transcription factor LEF1, and turns on expression of target genes. There are many Wnt-controlled target genes; c-Myc, a multifunctional regulator gene with roles in cellular transformation, is an example.

3.2 A more detailed look at Wnt signaling

In the Goentoro, et al. paper we are reading in class, we take a more detailed look of Wnt signaling beyond the cartoon in Fig. 2. The model is based on the work in Lee, et al. from the very first issue of *PLoS Biology*. Their schematic of Wnt signaling is shown in Fig. 3. They have labeled protein-protein interactions with arrows, each one identified with a number, with dashed arrows meaning interactions that are mediated through other proteins. Importantly, they have labeled subprocesses within this spaghetti-looking network to give it clarity. The destruction core cycle

of β-catenin cycles along, provided the equilibrium described by reactions 4 and 5 is unperturbed. The presence of a Wnt molecule affects this equilibrium by activating Dishevelled, which affects the reaction 4/5 equilbrium by breaking down the inactive APC/Axis, GSK-3 complex.

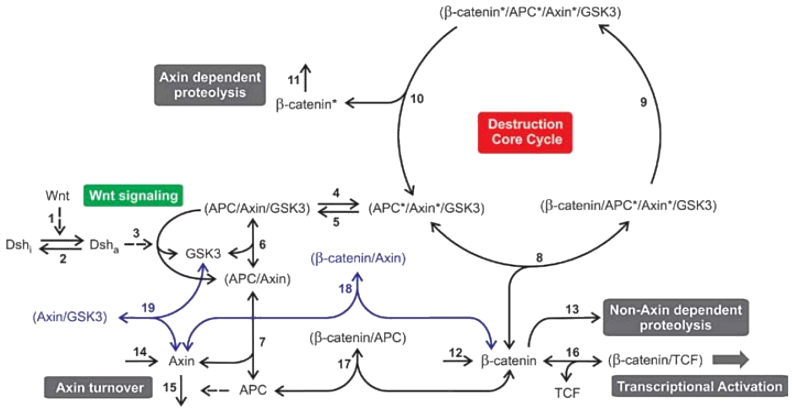

Figure 3: A more detailed model for Wnt signaling. Two headed arrows indicate reversible reactions and one-headed indicate irreversible reactions. Dashed arrows indicate reactions that have other mediators of the reactions. From Lee, et al., *PLoS Biology*, **1**, 116–132, 2003.

This is a complicated picture. Our goal is to mathematize this picture using the principle of mass action we talked about in the last lecture, get measured or estimated values for the parameters in the dynamical equations, and compute how changes in Wnt levels affect transcriptional activation.

3.3 Mathematizing the cartoon

As is often done in the study of signal transduction networks, **mass action kinetics** are used to model the dynamics. Recalling from last lecture, the rate of a chemical reaction is proportional to the product of the concentrations of the chemical species involved. The constant of proportionality is called the rate constant. Importantly, mass action kinetics do not consider individual reactant molecules, only concentrations of them. Bear in mind also when mass action is valid based on the assumptions we made when deriving it. When the number of reactants are small, or indeed their production is inherently stochastic, as in bursty gene expression, we should instead use stochastic simulation. Because we are not taking into account spatial arrangements of the molecules in our mass action treatment, we are implicitly making a **well-mixed assumption**, meaning that the concentrations are spatially homogeneous, or at least effectively so. Clearly, phosphorylated Dishevelled is not uniformly distributed in space, since it localizes to Frizzled/LRP on the membrane. Nonetheless, we assume that the dynamics of diffusion and spatial organization are fast com-

pared to the chemical kinetics, so we neglect the spatial distribution of molecules. (In future studies, we will not neglect diffusion, to interesting consequences.)

Despite all of these caveats, mass action kinetics seem to be unreasonably effective at describing measured dynamics and making testable predictions. We will therefore employ them in mathematizing the cartoon of the Wnt signaling pathway.

Lee and coworkers write dynamical equations for the entirety of the cartoon, making simplifying assumptions along the way. For demonstration purposes, we will mathematize only the β-catenin destruction core cycle with β-catenin input and phosphorylated β-catenin output. I.e., we will disconnect it from the reversible phosphorylation of APC (reactions 4 and 5 in Fig. 3). Note that reactions 4 and 5 are obviously crucial for getting the full dynamics of Wnt signaling.

In writing the dynamical equations, we do as Lee, et al. and assign numbers for the complexes, since "(β-catenin*/APC*/Axin*/GSK3)" is a bit big for a subscript!

number	**species**
3	APC*/Axin*/GSK-3
8	β-catenin/APC*/Axin*/GSK-3
9	β-catenin*/APC*/Axin*/GSK-3
10	β-catenin*
11	β-catenin

Now we can write down the differential equations using mass action.

$$\frac{\mathrm{d}c_3}{\mathrm{d}t} = -k_8 c_3 c_{11} + k_{-8} c_8 + k_{10} c_9, \tag{3.1}$$

$$\frac{\mathrm{d}c_8}{\mathrm{d}t} = k_8 c_3 c_{11} - k_{-8} c_8 - k_9 c_8, \tag{3.2}$$

$$\frac{\mathrm{d}c_9}{\mathrm{d}t} = k_9 c_8 - k_{10} c_9, \tag{3.3}$$

$$\frac{\mathrm{d}c_{10}}{\mathrm{d}t} = k_{10} c_9 - k_{11} c_{10}, \tag{3.4}$$

$$\frac{\mathrm{d}c_{11}}{\mathrm{d}t} = k_{12} - k_8 c_3 c_{11} + k_{-8} c_8. \tag{3.5}$$

We see that

$$\frac{\mathrm{d}c_3}{\mathrm{d}t} + \frac{\mathrm{d}c_8}{\mathrm{d}t} + \frac{\mathrm{d}c_9}{\mathrm{d}t} = 0, \tag{3.6}$$

which implies that the quantity $c_3 + c_8 + c_9$ is conserved. This makes sense, since this is the total amount of APC/Axin/GSK-3 present. We will call this conserved quantity c_A.

3.3.1 The unique steady state

We can solve for the steady state of this system of ODEs by setting the time derivatives equal to zero and solving. We can subtract equation (3.1) from equation (3.5) and solve to get that $c_9 = k_{12}/k_{10}$ at steady state. Then, using equations (3.2) and (3.4), we get $c_8 = k_{12}/k_9$ and $c_{10} = k_{12}/k_{11}$ at steady state. We then find that at steady state

$$c_3 = c_A - c_8 - c_9 = c_A - \frac{k_{12}}{k_9} - \frac{k_{12}}{k_8}. \tag{3.7}$$

We finally can solve for c_{11} at steady state to get

$$c_{11} = \frac{k_{12}}{k_8}\left(1 - \frac{k_{-8}}{k_9}\right)\left(c_A - \frac{k_{12}}{k_9} - \frac{k_{12}}{k_8}\right)^{-1}. \tag{3.8}$$

So, we have found a unique steady state. That the steady state exists and is unique is a useful piece of information in and of itself. We have also found that the steady state values of all species depend on the production rate of β-catenin, k_{12}.

3.3.2 Numerical solution

A system of linear ODEs is easily solved numerically. In solving the ODEs, we take an initial condition of no β-catenin at all in the system, starting only with Axin complex. The total concentration of Axin complex is conserved, with a level of 50 nM, as given in the Lee, et al. paper. We take all other parameters as those reported in the paper as well. The two parameters that are not reported there are k_{-8} and k_{12}. (Actually, k_8 is not reported either, but $K_{d,8} = k_{-8}/k_8$ is reported.)

It is easiest to see the effects of varying k_{12} and k_{-8} using interactive plotting. I do this, and demonstrate methods for numerically solving ODEs, in this Jupyter notebook. You will need to have a working Python 3 distribution with recent versions of JupyterLab, NumPy, SciPy, Pandas, and Bokeh installed.

A sample of the plot is shown in Fig. 4. In moving the sliders in the interactive plot, we see that k_{12} serves to set the scale of β-cat and β-cat* concentrations. Varying k_{-8} sets the total amount of β-catenin. Interestingly, for these parameter values, the concentrations of all Axin-associated complexes is essentially constant. We could make this approximation in the dynamics and get simplified equations for the kinetics.

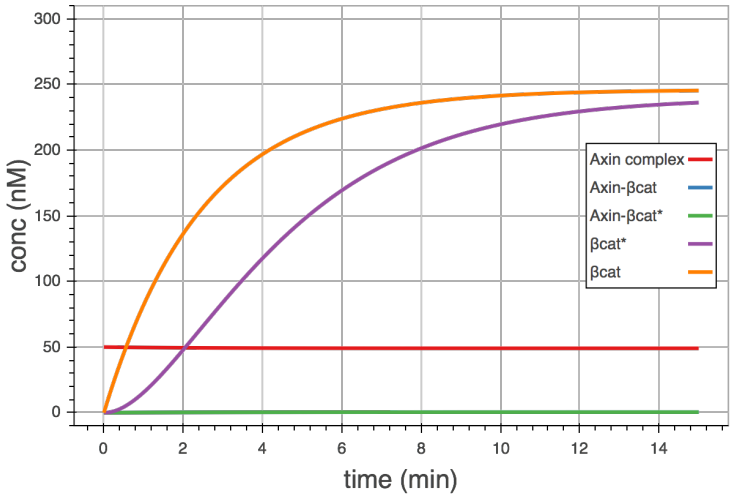

Figure 4: The dynamics of the major species in the β-catenin destruction cycle with all parameters as given in Lee, et al., and $k_{\text{-}8} = 1$ min^{-1} and $k_{12} = 100$ (nM-min)$^{-1}$.

4 Reaction-diffusion based patterns

In class, we will read a paper dealing with bone morphogenic protein (BMP) signaling. In order for biochemical signals to shape an organism, the signaling molecules themselves[3] need to be distributed in a spatially inhomogeneous way. It is not difficult to imagine that the biochemical cues would operate in a concentration-dependent manner; higher concentrations result in stronger signals than lower concentrations. Such chemical species, which determine cell fate in a developmental context in a concentration-dependent way, are called **morphogens**.

For this lecture, we will discuss **reaction-diffusion** mechanisms for generating spatial distributions of morphogens. This is important both practically and historically. Before we proceed in this lecture, I will highlight a couple things we will not cover. First, we will more carefully derive the reaction-diffusion equations when we get to our lectures on continuum mechanics, so we will more or less state them without proof here. Second, we will focus on a specific type of pattern, called *Turing patterns*, that arise from reaction-diffusion mechanisms. We will not talk much about a scaled morphogen gradient that is the subject of the Ben-Zvi et al. paper, but the fundamental mechanism, simply having diffusing and reacting species, is the same.

4.1 Turing's thoughts on reaction-diffusion mechanisms for morphogenesis

In my favorite paper of all time, Alan Turing (yes, *that* Alan Turing) laid out a prescription for morphogenesis. He described what should be considered when studying the "changes of state" of a developing organism. Turing said,

> In determining the changes of state one should take into account:
>
> (i) the changes of position and velocity as given by Newton's laws of motion;
>
> (ii) the stresses as given by the elasticities and motions, also taking into account the osmotic pressures as given from the chemical data;
>
> (iii) the chemical reactions;
>
> (iv) the diffusion of the chemical substances (the region in which this diffusion is possible is given from the mechanical data).

He proceeded to state, a few lines later, "The interdependence of the chemical and mechanical data adds enormously to the difficulty, and attention will therefore be confined, so far as is possible, to cases where these can be separated."

[3] Note that these cues could even have trivial signaling pathways; they can be transcription factors themselves.

In the second half of the class, we will attempt this difficult task of bringing together the chemical and the mechanical. For now, though, we will consider only chemical reactions and diffusion, and we will see that these together can produce patterns useful in development.

4.2 Reaction-diffusion equations for a single component

The reaction-diffusion equations are statements of conservation of mass. We will get into conservation laws in more depth later in the course, but for today we will take the equation describing the continuum conservation law as given.

Consider a chemical species i with diffusion coefficient D_i. Recall that the diffusion coefficient has dimension of L^2/T, or length squared over time. The concentration, a function of position x and time t, is $c_i(x,t)$. Then, the **flux** of species i in the x-direction due to diffusion, j_i is given by Fick's First Law,

$$j_i = -D_i \frac{\partial c_i}{\partial x}. \tag{4.1}$$

In investigating this equation, we see that flux has units of number of particles per area per time, N/L^2T. So, a flux, sometimes referred to as a *current*, is the number of particles that pass through a unit cross sectional area per unit time.

As we will derive in our discussions on continuum mechanics, the rate of change of concentration per unit time due to diffusion is given by the derivative[4] of the flux, as given by Fick's Second Law.

$$\frac{\partial c_i}{\partial t} = D_i \frac{\partial^2 c_i}{\partial x^2}. \tag{4.2}$$

This functional form makes sense intuitively. Imagine there is a local area of high concentration. By diffusion, the concentration at this point will drop, and it will rise away form the high concentration region. The second derivative of the concentration profile at the peak is negative, so the time derivative is also negative, which means that the concentration decreases there. The second derivative is positive away from the peak, so the concentration will rise in those regions.

Let $r_i(c_i)$ be the rate of production of species i by chemical reaction. Then, the rate of change of c_i due to chemical reaction is

$$\frac{\partial c_i}{\partial t} = r_i(c_i). \tag{4.3}$$

If we couple the chemical reactions with diffusion, we get

$$\frac{\partial c_i}{\partial t} = D_i \frac{\partial^2 c_i}{\partial x^2} + r_i(c_i). \tag{4.4}$$

[4] Actually, in 3D, the divergence.

This generalizes to two or three dimensions and multiple species.

$$\frac{\partial c_i}{\partial t} = D_i \nabla^2 c_i, + r_i(\mathbf{c}), \tag{4.5}$$

where

$$\nabla^2 = \frac{\partial^2}{\partial x^2} + \frac{\partial^2}{\partial y^2} + \frac{\partial^2}{\partial z^2}, \tag{4.6}$$

in three dimensional Cartesian coordinates, for example, and $\mathbf{c}$ is an array of the concentrations of all biochemical species.

4.3 Example: the Bicoid gradient

Bicoid was the first morphogen discovered. This morphogen can bind both DNA and RNA and is involved in transcriptional and translational regulation. It is present in high concentrations at the anterior regions of a *Drosophila* embryo and decays away as we move toward the posterior. It it thought that the gradient is set up by a reaction-diffusion process. In the most commonly used model, the reactions are simple.

1. Bicoid degrades with some characteristic degradation rate, γ.
2. *Bicoid* mRNA is tightly localized to the anterior of the embryo. Bicoid protein is continuously produced from this localized mRNA. To take into account the production and localization, we write this part of the chemical reaction as $q_0 f(x)$, where $f(x)$ is a dimensionless function describing the localization of the *bicoid* mRNA and therefore the Bicoid source.

Thus, $r(c,x) = -\gamma c + q_0 f(x)$. As already implied by our definition of Bicoid production, we will study this system in one dimension. The complete reaction diffusion equation is then

$$\frac{\partial c}{\partial t} = D \frac{\partial^2 c}{\partial x^2} - \gamma c + q_0 f(x). \tag{4.7}$$

If we are interested in the steady state Bicoid concentration profile, we set $\partial c/\partial t = 0$, giving

$$\frac{\partial^2 c}{\partial x^2} - \frac{\gamma}{D} c = -\frac{q_0}{D} f(x). \tag{4.8}$$

Let $\lambda = \sqrt{D/\gamma}$ be the characteristic length scale and let $\tilde{x} = x/\lambda$. We then have

$$\frac{\partial^2 c}{\partial x^2} - c = -\frac{q_0}{\gamma} f(\tilde{x}). \tag{4.9}$$

Importantly, when we nondimensionalize this way, we see that q_0/γ sets the scale of the concentration profile. We see further that, provided the source of Bicoid is sufficiently localized, λ is the only length scale in the problem and therefore must set the scale of the concentration gradient.

We can solve this equation in Fourier space as

$$\hat{c}(k) = \frac{q_0}{\gamma} \frac{\hat{f}(k)}{1+k^2}. \tag{4.10}$$

We can then easily solve this numerically with FFTs. We have only to specify $f(\tilde{x})$. We will choose $f(\tilde{x}) = 1 - \theta(\tilde{x} - a)$, where $\theta(x)$ is the Heaviside step function. In other words, we assume that the *bicoid* mRNA is localized in a region of size a at the anterior, given a source of Bicoid protein of width a. The result is shown in Fig. 5 with $a = 0.1$ (remember, the x-axis is in units of λ.).

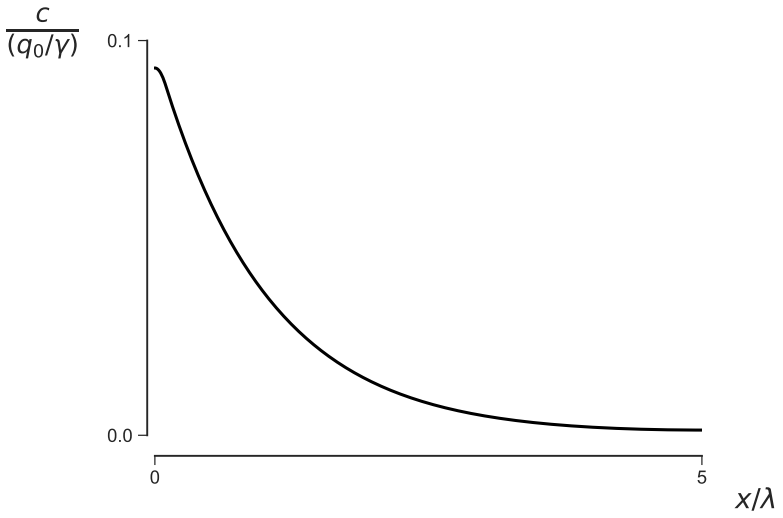

Figure 5: The gradient of Bcd.

This method of modeling the source of Bcd is useful, but another commonly used method is to consider a constant flux of Bcd at the anterior. In this case, the dynamical equations for the profile are

$$\frac{\partial c}{\partial t} = D \frac{\partial^2 c}{\partial x^2} - \gamma c, \tag{4.11}$$

$$j(x=0) = -D \left.\frac{\partial c}{\partial x}\right|_{x=0} = j_0. \tag{4.12}$$

We also have a **no flux** condition on the posterior end of the embryo, such that

$$j(x=L) = -D \left.\frac{\partial c}{\partial x}\right|_{x=L} = 0. \tag{4.13}$$

The no flux conditions ensures conservation of mass; no material can flow out of the end of the embryo. At steady state, we have

$$D\frac{\partial^2 c}{\partial x^2} - \gamma c = 0, \tag{4.14}$$

which has solution

$$c(x) = c_1 e^{-x/\lambda} + c_2 e^{x/\lambda}, \tag{4.15}$$

with again $\lambda = \sqrt{D/\gamma}$, and c_1 and c_2 being constants of integration. Using the boundary conditions (4.12) and (4.13), we can solve for c_1 and c_2 to get (after some algebra) a steady state concentration profile of

$$c(x) = \frac{j_0}{\sqrt{D\gamma}}\left(e^{-x/\lambda} + \frac{\cosh\frac{x}{\lambda}}{\sinh\frac{L}{\lambda}}e^{-L/\lambda}\right). \tag{4.16}$$

In *Drosophila*, the Bcd concentration is decays to zero about half way along the anterior-posterior axis of the embryo, so $L \gg \lambda$. When this is the case, the second term in the expression for the concentration profile is small, so

$$c(x) \approx \frac{j_0}{\sqrt{D\gamma}} e^{-x/\lambda}. \tag{4.17}$$

4.4 Scaling of the Bcd gradient

Note that the reaction-diffusion mechanism we considered for the Bicoid gradient does not allow for **scaling**. A system exhibits scaling, or is scale invariant, if the pattern does not change if the overall system size changes. Think of it like this: imagine a two-dimensional square zebra and another one twice its size. If the mechanism that generates stripes exhibits scaling, these two zebras will have the same number of stripes. Similarly, flags scale; a tiny American flag has the same pattern as a giant one.

Mathematically, if we non-dimensionalized x by the total length of the system (organism), then the length would not appear at all in the system. Clearly this is not the case for the proposed model of Bicoid, since the natural length scale is λ. Indeed, defining $\tilde{x} = x/L$, we have

$$c(\tilde{x}) = \frac{j_0}{\sqrt{D\gamma}} e^{-\tilde{x}L/\lambda}, \tag{4.18}$$

with L appearing explicitly in the concentration profile.

In the Ben-Zvi paper, the authors discuss a mechanism for scaling of a similar gradient, that of BMP in dorsal-ventral patterning in a *Xenopus* embryo. In your homework associated with that paper, you will explore other means of scaling.

4.5 Reaction-diffusion equations for multiple components

As mentioned before, the equations for reaction-diffusion dynamics generalize to multiple components. Let $\mathbf{c} = \{c_1, c_2, \ldots\}$ be the concentrations of each of n total species. Then, we can write

$$\frac{\partial c_i}{\partial t} = D_i \nabla^2 c_i, + r_i(\mathbf{c}). \tag{4.19}$$

Here, we have assumed that the diffusion of each species is independent of that of all others. The chemical reaction rates, though, may depend on other species.

In the study of many signaling studies, authors often make the **well-mixed approximation**, and neglect the diffusion term and any spatial dependence on the chemical components. In the next section, we will see beautiful patterns emerge from reaction-diffusion with two chemical species. These patterns are called **Turing patterns**.

4.6 Turing patterns two-component R-D systems

Consider two chemical species that can undergo diffusion in one dimension (for simplicity). Then, the reaction-diffusion equations for these species are

$$\frac{\partial a}{\partial t} = D_a \frac{\partial^2 a}{\partial x^2} + r_a(a, s), \tag{4.20}$$

$$\frac{\partial s}{\partial t} = D_s \frac{\partial^2 s}{\partial x^2} + r_s(a, s), \tag{4.21}$$

where we have denoted the concentration of the two species to be a and s. To have a concrete example in mind, since this often helps understanding, we will take

$$r_a = \rho a^2 s - \gamma a \tag{4.22}$$

$$r_s = \beta - \rho a^2 s \tag{4.23}$$

This means that a serves as an activator and s is an inhibitor. We can see this by looking at each term. The $\rho a^2 s$ term means that a is catalyzes its own production, but needs a substrate enzyme to do so. The appearance of the $-\rho a^2 s$ term means that the substrate is consumed in this process. The activator undergoes autodegradation (the $-\gamma a$ term), and the substrate is produced at a constant rate β. We could include autodegradation of the substrate, but we assume that that process is very slow compared to the other processes at play and neglect it for simplicity. This model is called the activator-substrate depletion model, or ASDM.

4.6.1 Nondimensionalization

As we have already seen, in studying dynamical systems, it is almost always a good idea to **nondimensionalize** them. In general, we can choose a units of time to be τ so that we can nondimensionalize time, $\tilde{t} = t/\tau$. We nondimensionalize position x as $\tilde{x} = \sqrt{D_s \tau}$ (a similar length scale that appeared in the Bicoid example). Then, the reaction diffusion system can be written as

$$\frac{\partial a}{\partial \tilde{t}} = d \frac{\partial^2 a}{\partial \tilde{x}^2} + \tau r_a(a, s), \tag{4.24}$$

$$\frac{\partial s}{\partial \tilde{t}} = \frac{\partial^2 s}{\partial \tilde{x}^2} + \tau r_s(a, s), \tag{4.25}$$

where the tildes represent dimensionless quantities and $d \equiv D_a/D_s$ is the ratio of the diffusive rates of the activator and substrate. This already shows us that the *ratio* of the diffusion coefficients will be an important parameter.

We are free to choose how we nondimensionalize the concentrations of the activator and substrate to get fully nondimensional dynamical equations. It is convenient to nondimenionalize using $\tau = 1/\gamma$, $a = \beta \tilde{a}/\gamma$, and $s = \gamma^2 \tilde{s}/\beta\rho$.

Thus, we can write the reaction-diffusion equations as

$$\frac{\partial a}{\partial t} = d \frac{\partial^2 a}{\partial x^2} + a^2 s - a \tag{4.26}$$

$$\frac{\partial h}{\partial t} = \frac{\partial^2 s}{\partial x^2} + \mu(1 - a^2 s), \tag{4.27}$$

where $\mu = \beta^2 \rho / k^3$, and we have dropped the tildes for notational convenience, knowing that all variables and parameters are dimensionless. Conveniently, we have gone from five parameters down to two.[5] So, the dynamics are governed by only two parameters, the ratio of the diffusion coefficients, d, and the ratio of production to degradation rates μ.

Going forward, in the general treatment of the two-component system, we will assume everything is properly nondimensionalized and write our dynamical equations as

$$\frac{\partial a}{\partial t} = d \frac{\partial^2 a}{\partial x^2} + r_a(a, s), \tag{4.28}$$

$$\frac{\partial s}{\partial t} = \frac{\partial^2 s}{\partial x^2} + r_s(a, s). \tag{4.29}$$

[5] We could actually arrive at the same dimensionless equations if we had a different ρ values, say ρ_a and ρ_s, for production of activator and depletion of substrate, bringing the parameter count from six down to two.

4.6.2 Homogeneous steady state

The reaction-diffusion system is at **steady state** when the time derivatives are zero. A steady state is **homogeneous** when the spatial derivatives are also zero. This just means that the concentration of all chemical species are spatially uniform. A homogeneous steady state (a_0, s_0) then satisfies $r_a(a_0, s_0) = r_s(a_0, s_0) = 0$. For the ASDM, the homogeneous steady state is $a_0 = s_0 = 1$ and is unique.

4.6.3 Linear stability analysis

Imagine the system is in the homogeneous steady state. What happens to this system if it experiences a small perturbation? This question can be addressed using **linear stability analysis**.

Let us expand both sides of our dynamical equations in a Taylor series about $(a, s) = (a_0, s_0)$.

$$\frac{\partial}{\partial t}(a_0 + \delta a) = d\,\frac{\partial^2}{\partial x^2}(a_0 + \delta a) + r_a(a_0, s_0) + r_{a,a}\,\delta a + r_{a,s}\,\delta s + \cdots, \tag{4.30}$$

$$\frac{\partial}{\partial t}(s_0 + \delta s) = \frac{\partial^2}{\partial x^2}(s_0 + \delta a) + r_s(a_0, s_0) + r_{s,a}\,\delta a + r_{s,s}\,\delta s + \cdots, \tag{4.31}$$

where $\delta a = a - a_0$ and $\delta s = s - s_0$. We also defined

$$r_{a,s} = \left.\frac{\partial r_a}{\partial a}\right|_{a_0,s_0}, \tag{4.32}$$

with other parameters similarly defined. Now, $r_a(a_0, s_0) = r_s(a_0, s_0) = 0$, since (a_0, s_0) is a homogeneous steady state, and all derivatives of a_0 and s_0 are also zero. Then, to linear order in the perturbation $(\delta a, \delta s)$, we have

$$\frac{\partial\,\delta a}{\partial t} = d\,\frac{\partial^2\,\delta a}{\partial x^2} + r_{a,a}\,\delta a + r_{a,s}\,\delta s, \tag{4.33}$$

$$\frac{\partial\,\delta s}{\partial t} = \frac{\partial^2\,\delta s}{\partial x^2} + r_{s,a}\,\delta a + r_{s,s}\,\delta s. \tag{4.34}$$

We can write the spatial variation in the perturbation as a Fourier series, with mode k being $\delta a_k(t)\mathrm{e}^{ikx}$. Then the dynamical equation for mode k is

$$\frac{\mathrm{d}\,\delta a_k}{\mathrm{d}t} = -dk^2\,\delta a_k + r_{a,a}\,\delta a_k + r_{a,s}\,\delta s_k, \tag{4.35}$$

$$\frac{\mathrm{d}\,\delta s_k}{\mathrm{d}t} = -k^2 + r_{s,a}\,\delta a_k + r_{s,s}\,\delta s_k. \tag{4.36}$$

This can be written in matrix form as

$$\frac{\mathrm{d}}{\mathrm{d}t}\begin{pmatrix}\delta a_k\\ \delta s_k\end{pmatrix} = \mathsf{A}\cdot\begin{pmatrix}\delta a_k\\ \delta s_k\end{pmatrix}, \tag{4.37}$$

where

$$\mathsf{A} = \begin{pmatrix}-dk^2 + r_{a,a} & r_{a,s}\\ r_{s,a} & -k^2 + r_{s,s}\end{pmatrix} \tag{4.38}$$

is the **linear stability matrix**. This is now a linear system of equations and the solution is

$$\begin{pmatrix}\delta a_k\\ \delta s_k\end{pmatrix} = c_1\mathbf{v}_1\mathrm{e}^{\sigma_1 t} + c_2\mathbf{v}_2\mathrm{e}^{\sigma_2 t}, \tag{4.39}$$

where σ_1 and σ_2 are the eigenvalues of A and $\mathbf{v}_1$ and $\mathbf{v}_2$ are the eigenvectors. So, if the real part of one of the σ's is positive, the kth mode of the perturbation will grow over time.

Remember that for a 2×2 matrix, the eigenvalues are

$$\sigma = \frac{1}{2}\left(\mathrm{tr}\,\mathsf{A} \pm \sqrt{\mathrm{tr}^2\mathsf{A} - 4\det\mathsf{A}}\right). \tag{4.40}$$

So, the real part of the largest eigenvalue is negative if the trace of the linear stability matrix is negative and its determinant is positive. Otherwise, the largest eigenvalue has a positive real part and the homogeneous steady state is not stable and patterns or oscillations can spontaneously emerge.

4.6.4 Consequences of linear stability analysis

We can write the trace and determinant explicitly.

$$\mathrm{tr}\,\mathsf{A} = -(1+d)k^2 + r_{a,a} + r_{s,s}, \tag{4.41}$$

$$\det\mathsf{A} = dk^4 - (r_{a,a} + dr_{s,s})k^2 + r_{a,a}r_{s,s} - r_{a,s}r_{s,a}. \tag{4.42}$$

In the absence of spatial information (and therefore diffusion), the trace is negative if and only if at least one of $r_{a,a}$ and $r_{s,s}$ is negative. This means that chemical reaction system by itself is stable. Interestingly, the trace is maximal for the zeroth mode, which means that an instability arising from the trace becoming positive has the zeroth mode as its fastest growing. If the determinant is positive at the onset of the instability (when the trace crosses zero), the eigenvalues are imaginary, which means that the zeroth mode is oscillatory. This is called a Hopf bifurcation.

For patterning in a developmental context, we want stable chemical reaction systems, and we would like patterns to be emergent as the organism grows. Note that the size of the embryo sets which values of k are allowed; the organism has to be big enough to fit the modes. So, an organism grows long enough to fit a mode for which the eigenvalue is positive, and then patterns spontaneously emerge. So, we generally do not want a Hopf bifurcation in development, which means that a necessary condition is that at least one of $r_{a,a}$ or $r_{s,s}$ is negative.

Now, the requirement that the chemical reaction system is stable in the absence of spatial information implies that $r_{a,a}r_{s,s} - r_{a,s}r_{s,a} > 0$. The determinant is convex and quadratic in k^2, so it has a minimum when

$$\frac{\partial^2}{\partial k^2} \det \mathsf{A} = 2dk^2 - r_{a,a} - dr_{s,s} = 0. \tag{4.43}$$

Therefore, the fastest growing mode in the instability is given by

$$k_0^2 = \frac{r_{a,a} + dr_{s,s}}{2d}. \tag{4.44}$$

This minimum occurs for real k_0 only in the presence of positive feedback, or, in chemical terms, if at least one of the species is autocatalytic, meaning that either $r_{a,a} > 0$ or $r_{s,s} > 0$ or both. We determined earlier that the condition of stable chemical reactions implies that at least one of these terms is negative, so we now have that exactly one must be positive and one must be negative. We arbitrarily pick $r_{a,a}$ to be autocatalyic (hence the name, "activator").

4.6.5 Linear stability analysis for the ASDM

For the ASDM, we have $r_{a,a} = r_{a,s} = 0$, $r_{s,a} = -2\mu$, and $r_{s,s} = -\mu$, giving

$$\mathsf{A} = \begin{pmatrix} 1 - dk^2 & 1 \\ -2\mu & -\mu - k^2 \end{pmatrix}. \tag{4.45}$$

The trace and determinant are

$$\operatorname{tr} \mathsf{A} = -(1+d)k^2 + 1 - \mu \tag{4.46}$$

$$\det \mathsf{A} = (dk^2 - 1)(\mu + k^2) + 2\mu = dk^4 - (1 - d\mu)k^2 + \mu. \tag{4.47}$$

So, in order to avoid the Hopf bifurcation, we need $\mu > 1$. The fastest growing mode is

$$k_0^2 = \frac{1 - d\mu}{2d}. \tag{4.48}$$

For k_0 to be real, we must have $d/\mu < 1$. Since $\mu > 1$, the condition for a Turing instability is that $d < 1$. This can be shown to be the case in general, not just for the ASDM. So, we have summarized the requirements for a Turing instability.

1. One species is autocatalytic ($r_{a,a} > 0$) and one is inhibitory ($r_{s,s} < 0$).
2. The inhibitory species (in the ASDM model, this is the substrate) must diffuse more rapidly than the activating species.

The intuition here is that the activator starts producing more of itself locally. The local peak starts to spread, but the inhibitor diffuses more quickly that pins the peak of activator in so that it cannot spread. This gives a set wavelength of the pattern of peaks.

4.6.6 Turing patterns do not scale

Turing patterns, such as those generated by the ASDM, do not scale because the wavelength of the pattern, given by the fastest growing mode, k, is independent of system size. So, if a system is twice as large, it would have twice as many peaks and valleys in the pattern.

5 Delta-Notch signaling

During development, cells need to communicate with their nearest neighbors to enable differentiation. The **Delta-Notch** pathway is central to this end. We will see this when we discuss the Soroldoni, et al. paper, in which Delta-Notch signaling couples genetic oscillators in neighboring cells.

5.1 Molecular biology of the Delta-Notch signaling system

Delta-Notch signaling provides a mechanism for neighboring cells to communicate with each other. The molecular mechanism is shown in Fig. 6. Notch is a transmembrane protein that is the receptor for another transmembrane protein Delta. When a cell is expressing Notch and its neighbor is expressing Delta, Delta binds Notch, which results in a conformational change. This enables proteolytic cleavage of Notch, resulting in the Notch intracellular domain (Nicd) detaching from the membrane complex. Nicd acts as a transcription factor. It is a co-activator with Mastermind and a co-repressor with Hairless, in addition to having other binding partners that control gene expression.

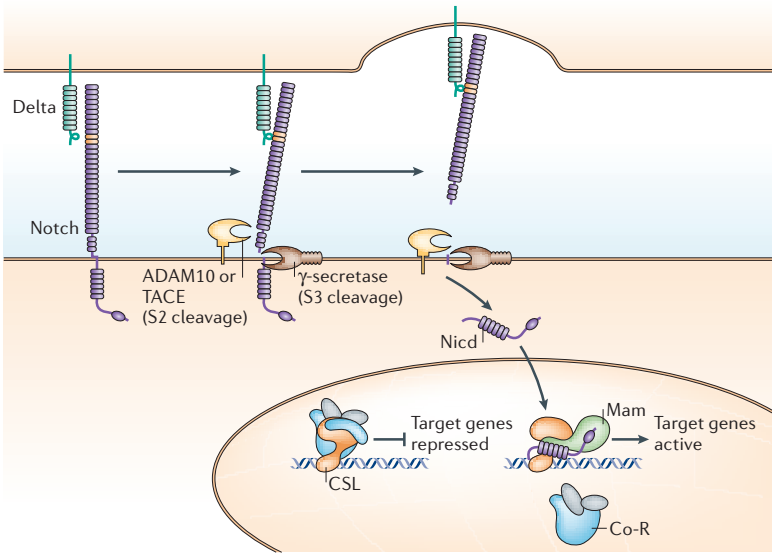

Figure 6: Sketch of the molecular details of Delta-Notch signaling. The insides of neighboring cells are shown in brown and the intercellular space is shown in light blue. Taken from Bray, *Nat. Rev. Mol. Cell Biol.*, **7**, 678–689, 2006.

Importantly, Nicd represses production of Delta. So, a cell that has a lot of cleaved Notch will stop producing Delta. Thus, a cell expressing a lot of Delta will

suppress Delta expression in the neighboring cell by activating Notch in the neighbor. A schematic of this process is shown in Fig. 7.

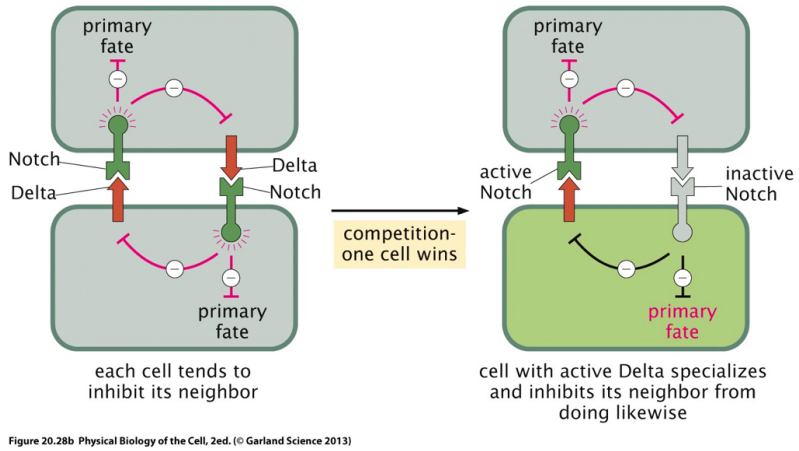

Figure 7: Schematic of nearest-neighbor cell differentiation by Delta-Notch. Delta expressed by the bottom cell activates Notch in the top cell. The activated Notch in the top cell suppresses Delta in the top cell. Because there is no Delta on the surface of the top cell, Notch is inactive in the bottom cell. Since Notch is inactive, Delta continues being expressed in the bottom cell.

So, the Delta-Notch system enables a cell to access a cell fate *and* instruct its neighbors *not* to access the same fate.

5.2 Mathematical analysis of the Delta-Notch system

We will develop a simple model to describe the dynamics of the Delta-Notch signaling between two nearest-neighbor cells. Let N_1 be the number of active Notch molecules in cell 1 and D_1 be the number of Delta molecules, with N_2 and D_2 similarly defined. We then write the dynamics as

$$\frac{dN_1}{dt} = F(D_2) - \gamma_N N_1 \tag{5.1}$$

$$\frac{dD_1}{dt} = G(N_1) - \gamma_D D_1 \tag{5.2}$$

$$\frac{dN_2}{dt} = F(D_1) - \gamma_N N_2 \tag{5.3}$$

$$\frac{dD_2}{dt} = G(N_2) - \gamma_D D_2. \tag{5.4}$$

We have defined γ_N and γ_D to be the respective autodegradation rates of Notch and Delta. The function $F(D)$ describes how the Delta level in a neighboring cell affects

the Notch level. This function should be monotonically increasing, since more Delta implies more active Notch. The function $G(N)$ describes how the level of active Notch in a cell affects its Delta level. Since Notch represses Delta, this should be monotonically decreasing.

5.2.1 Nondimensionalization

We will **nondimensionalize** these dynamical equations. this is the process of re-defining variables and parameters so that each term in the system of ODEs has no units. This also usually results in driving down the total number of parameters. We define the following, with dimensionless quantities being either lowercase or marked with a tilde.

$$t = \tau \tilde{t} \tag{5.5}$$

$$G(N_2) = G_0\, g(N_2/N_0) \tag{5.6}$$

$$F(D_2) = F_0 f(D_2/D_0) \tag{5.7}$$

$$N_1 = N_0 n_1 \tag{5.8}$$

$$D_1 = D_0 d_1, \tag{5.9}$$

with other variables similarly defined. After substitution and rearrangement, we get

$$\dot{n}_1 = \frac{F_0\,\tau}{N_0} f(d_2) - \gamma_N \tau n_1 \tag{5.10}$$

$$\dot{d}_1 = \frac{G_0\,\tau}{D_0}\, g(n_1) - \gamma_D \tau d_1 \tag{5.11}$$

$$\dot{n}_2 = \frac{F_0\,\tau}{N_0} f(d_1) - \gamma_N \tau n_2 \tag{5.12}$$

$$\dot{d}_2 = \frac{G_0\,\tau}{D_0}\, g(n_2) - \gamma_D \tau d_2, \tag{5.13}$$

where the over-dot indicates differentiation by $\tilde{t}$. Now, we choose $\tau = \gamma_N^{-1}$ and N_0 and D_0 such that $\lim_{d\to\infty} f(d) = 1$ and $g(n = 0) = 1$. We further choose $F_0 = N_0/\tau$ and $G_0 = D_0/\tau$. With these choices, we have

$$\dot{n}_1 = f(d_2) - n_1 \tag{5.14}$$

$$\dot{d}_1 = \nu\,(g(n_1) - d_1) \tag{5.15}$$

$$\dot{n}_2 = f(d_1) - n_2 \tag{5.16}$$

$$\dot{d}_2 = \nu \left(g(n_2) - d_2 \right), \tag{5.17}$$

where we are left with a single parameter, $\nu = \gamma_D / \gamma_N$, the ratio of the decay rates of Delta and Notch.

5.2.2 Homogeneous steady state

We are interested in knowing if these two neighboring cells can differentiate from each other. We therefore wish to find a homogeneous steady state, $n_1 = n_2 = n_0$ and $d_1 = d_2 = d_0$, and test its stability. If this homogeneous steady state is unstable (i.e, if the dynamical system "runs away" from the homogeneous steady state upon a small perturbation), we expect the cells to be able to differentiate. If it is stable, they cannot spontaneously differentiate.

To find the steady state, we solve the system of equations with all time derivatives set to zero. I.e., we wish to solve

$$f(d_0) - n_0 = 0, \tag{5.18}$$

$$g(n_0) - d_0 = 0. \tag{5.19}$$

The first equation gives $n_0 = f(d_0)$, so the second equation tells us we must have $g(f(d_0)) = d_0$. We will write $g(f(x))$ as $gf(x)$, where $gf(x)$ is called the **composition** of the functions g and f. Now, $f(x)$ is a monotonically increasing function and $g(x)$ is a monotonically decreasing function, so $gf(x)$ is a monotonically decreasing function. So we have that $gf(d_0)$ is monotonically decreasing toward zero while the function $h(d_0) = d_0$ is monotonically increasing from zero. This means that these two functions cross exactly once, so there exists a *unique* homogeneous steady state.

5.2.3 Linear stability analysis

To test the stability of the homogeneous steady state, we turn to **linear stability analysis**. The basic idea is to linearize the right hand sides of the ODEs by expanding them in Taylor series to first order about the homogeneous steady state. The result is a linear dynamical system which is readily solved by computing the eigenvalues. If any of the real parts of the eigenvalues is positive, the homogeneous steady state is unstable, since the concentration of one of the species will, at least close to the homogeneous steady state, grow exponentially.

Let n_0, d_0 be the homogeneous steady state. We take a small perturbation off of this steady state such that

$$n_1 = n_0 + \delta n_1 \tag{5.20}$$

$$d_1 = d_0 + \delta d_1 \tag{5.21}$$

$$n_2 = n_0 + \delta n_2 \tag{5.22}$$

$$d_1 = d_0 + \delta d_2, \tag{5.23}$$

where $\mathbf{u} \equiv (\delta n_1, \delta d_1, \delta n_2, \delta d_2)$ is a small perturbation about the homogeneous steady state. We expand the functions $f(d)$ and $g(n)$ to first order in the perturbation.

$$f(d_2) = f(d_0) + f'(d_0)\,\delta d_2 + \mathcal{O}\left((\delta d_2)^2\right), \tag{5.24}$$

$$g(n_1) = g(n_0) + g'(n_0)\,\delta n_1 + \mathcal{O}\left((\delta n_1)^2\right), \tag{5.25}$$

and so on. We define $f_0 = f'(d_0)$ and $g_0 = g'(n_0)$ for notational convenience. Then, to linear order in the perturbation, we have

$$\frac{\mathrm{d}}{\mathrm{d}t}\,\delta n_1 = f_0\,\delta d_2 - \delta n_1 \tag{5.26}$$

$$\frac{\mathrm{d}}{\mathrm{d}t}\,\delta d_1 = \nu\,(g_0\,\delta n_1 - \delta d_1) \tag{5.27}$$

$$\frac{\mathrm{d}}{\mathrm{d}t}\,\delta n_2 = f_0\,\delta d_1 - \delta n_2 \tag{5.28}$$

$$\frac{\mathrm{d}}{\mathrm{d}t}\,\delta d_2 = \nu\,(g_0\,\delta n_2 - \delta d_2)\,. \tag{5.29}$$

This can be written in matrix form as

$$\frac{\mathrm{d}}{\mathrm{d}t}\,\mathbf{u} = \mathsf{A}\cdot\mathbf{u}, \tag{5.30}$$

with

$$\mathsf{A} = \begin{pmatrix} -1 & 0 & 0 & f_0 \\ \nu g_0 & -\nu & 0 & 0 \\ 0 & f_0 & -1 & 0 \\ 0 & 0 & \nu g_0 & -\nu \end{pmatrix}. \tag{5.31}$$

It is useful to remember that the sum of the eigenvalues of a matrix is given by the trace and the product of the eigenvalues is given by the determinant.

$$\operatorname{tr}\mathsf{A} = -2(1+\nu) \tag{5.32}$$

$$\det\mathsf{A} = \nu^2\left(1 - f_0^2 g_0^2\right). \tag{5.33}$$

We can directly compute the eigenvalues by computing the characteristic polynomial.

$$(1+\lambda)^2(\nu+\lambda)^2 - \nu^2 f_0^2 g_0^2 = 0 \tag{5.34}$$

Therefore, one pair of eigenvalues is given by the solutions of

$$(1+\lambda)(\nu+\lambda) = \nu f_0 g_0, \tag{5.35}$$

and the other pair by solutions of

$$(1+\lambda)(\nu+\lambda) = -\nu f_0 g_0. \tag{5.36}$$

These are all quadratic equations, which can be solved to give

$$\lambda_1 = -\frac{1+\nu}{2}\left(1+\sqrt{1-\frac{4\nu}{(1+\nu)^2}(1-f_0 g_0)}\right), \tag{5.37}$$

$$\lambda_2 = -\frac{1+\nu}{2}\left(1-\sqrt{1-\frac{4\nu}{(1+\nu)^2}(1-f_0 g_0)}\right), \tag{5.38}$$

$$\lambda_3 = -\frac{1+\nu}{2}\left(1+\sqrt{1-\frac{4\nu}{(1+\nu)^2}(1+f_0 g_0)}\right), \tag{5.39}$$

$$\lambda_4 = -\frac{1+\nu}{2}\left(1-\sqrt{1-\frac{4\nu}{(1+\nu)^2}(1+f_0 g_0)}\right). \tag{5.40}$$

Clearly, eigenvalues λ_1 and λ_3 have negative real parts. For λ_2 to have a positive real part, we must have

$$f_0 g_0 > 1. \tag{5.41}$$

This is not possible since recall that $f_0 > 0$ and $g_0 < 0$, so $f_0 g_0 < 0$. So, the only eigenvalue that can have positive real part is λ_4. This happens when

$$f_0 g_0 < -1. \tag{5.42}$$

This condition must be met for the homogeneous steady state to be unstable. This tells us that either $f(d)$, $g(n)$, or both must be steep functions near the steady state. This implies cooperativity, which we will discuss more explicitly in a simple limit in section 5.2.5.

5.2.4 Linear stability in the $\nu \gg 1$ regime

To make more analytical progress, we consider the case where $\nu \gg 1$, which is to say that the Delta dynamics are much faster than the Notch dynamics. We note that the terms multiplying ν in equations (5.15) and (5.17) must be of order $\nu^{-1} \approx 0$, since all of the variables have been scaled to unity. This means that $g(n_1) \approx d_1$ and

$g(n_2) \approx d_2$. With this approximation, we can reduce the dynamical system to two equations.

$$\dot{n}_1 = fg(n_2) - n_1 \tag{5.43}$$

$$\dot{n}_2 = fg(n_1) - n_2. \tag{5.44}$$

We can again perform linear stability analysis, defining now

$$fg_0 \equiv \left.\frac{\mathrm{d}fg(n)}{\mathrm{d}n}\right|_{n=n_0}. \tag{5.45}$$

We get

$$\frac{\mathrm{d}}{\mathrm{d}t}\begin{pmatrix}\delta n_1 \\ \delta n_2\end{pmatrix} = \begin{pmatrix}-1 & fg_0 \\ fg_0 & -1\end{pmatrix} \cdot \begin{pmatrix}\delta n_1 \\ \delta n_2\end{pmatrix}. \tag{5.46}$$

The sum of the eigenvalues of this linear stability matrix is $\lambda_1 + \lambda_2 = -2$, implying that at least one of the eigenvalues has a negative real part. The product of the eigenvalues is given by the determinant, or $\lambda_1\lambda_2 = 1 - (fg_0)^2$. Since at least one of the eigenvalues has a negative real part, we must have $\lambda_1\lambda_2 < 0$ to have an instability. So, we must have $(fg_0)^2 > 1$, or $fg_0 < -1$, since $fg_0 < 0$. This tells us that the composite function $fg(x)$ must be steep.

5.2.5 Cooperativity in the $\nu \gg 1$ regime

We will model $f(x)$ and $g(x)$ as Hill functions to gain some more insights into the requirements for instability.

$$f(x) = \frac{x^{n_f}}{a + x^{n_f}}, \tag{5.47}$$

$$g(x) = \frac{b}{b + x^{n_g}}. \tag{5.48}$$

Then, we have

$$fg(x) = \frac{[b/(b + x^{n_g})]^{n_f}}{a + [b/(b + x^{n_g})]^{n_f}}. \tag{5.49}$$

From this, we can compute fg_0 as

$$fg_0 = \left.\frac{\mathrm{d}fg}{\mathrm{d}x}\right|_{x=x_0} = -\frac{an_f n_g}{b}\,\frac{x_0^{n_g-1}\left[b/(b + x_0^{n_g})\right]^{n_f+1}}{\left(a + \left[b/(b + x_0^{n_g})\right]^{n_f}\right)^2}, \tag{5.50}$$

where we are calling x_0 the homogeneous steady state. We compute the differential of this function for $n_f = n_g = 1$.

$$fg_0 = -\frac{a^2 b^2}{(b + ab + ax_0)^2}. \tag{5.51}$$

Thus, we have that fg_0 can never have a magnitude greater than unity. Therefore, if $n_f = n_g = 1$, we cannot have an instability. So, a requirement for instability of the Delta-Notch system in the limit where Delta dynamics are much faster than Notch dynamics is that we must have cooperativity, i.e., $n_f > 1$, $n_g > 1$, or both.

6 Segmentation clocks

The precursor to vertebrae are called *somites*, illustrated in Fig. 8. In this lecture, we explore the mechanisms for **somitogenesis**, the process by which these somites are formed.

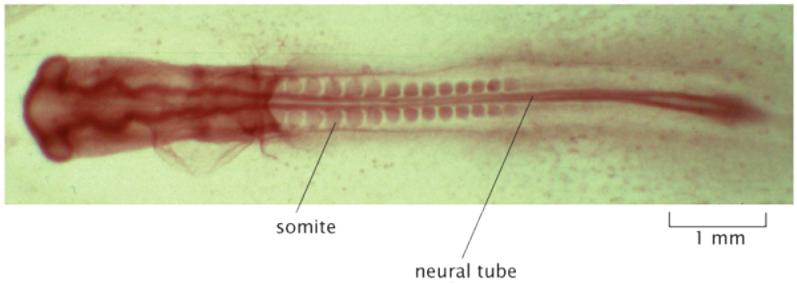

Figure 8: Somites in a developing chick embryo. Image taken from Phillips, et al., *Physical Biology of the Cell*, 2nd Ed., Fig. 20.21, 2012.

6.1 Basics of somitogenesis

It is believed that somitogenesis happens as a result of oscillatory gene expression and arrest of this oscillation at a specified position along the anterior-posterior axis of the developing embryo. At the tail end of the embryo, cells in the presomitic mesoderm (PSM) (Fig. 9) exhibit oscillatory expression of certain genes. In zebrafish, these genes are *her1* and *her7*, related to the pair-rule gene *hairy* in *Drosophila* (hence the name; *her* is short for *hairy-related*). As the *her* genes oscillate, the organism is growing, so the PSM keeps moving posteriorly. If the oscillating cells are far enough from the posterior, they arrest. The position where the arrest occurs is called the **arrest front**. If a cell is in a peak of the *her* oscillation when it arrests, it will have one fate, but if it is in a valley, it will have another fate. Thus, the alternating structure of the somites is formed. Note that the distance between the arrest front and the posterior end of the organism may fluctuate, but in many models is taken to be constant.

6.2 The clock-and-wavefront model

The **clock-and-wavefront model** was proposed by Cooke and Zeeman in 1975 and was one of the first models put forward to describe somitogenesis. This model is based on the following assumptions.

a) All cells in the PSM are oscillating.

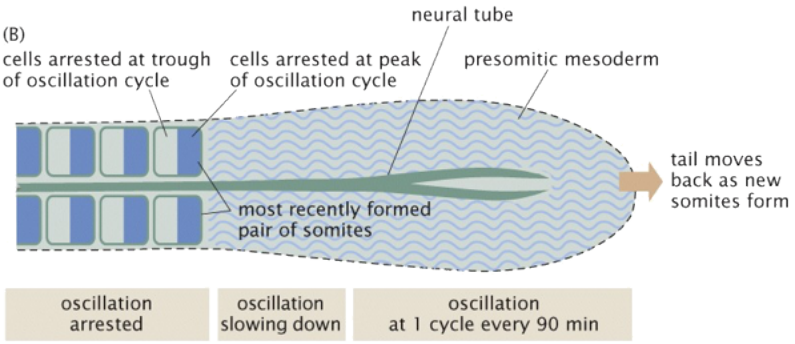

Figure 9: A schematic of the clock and wavefont model for somitogenesis. Image taken from Phillips, et al., *Physical Biology of the Cell*, 2nd Ed., 2012.

b) Coupling between the cells induces synchrony in oscillation, setting the oscillation frequency to be T.

c) Waves arrest at a front at the anterior.

d) The arrest front moves posteriorly with a speed v.

In this model, since all cells in the PSM are oscillating *in unison*, meaning that they have both the same frequency and the same phase, the dynamics of the extension of the PSM during growth is irrelevant. Only the motion of the front into the oscillating cells is important.

An important conclusion of this model is that the size of the somites is $s = vT$. This is the distance traveled by the arrest front between peaks in the oscillators. The model can be tested indirectly by measuring somitogenesis over a time interval of set length, as shown in Fig. 10. We measure the length of the region of somites, D_s, and the position of the arrest front, W_a and W_b and the beginning and end of the time interval, respectively.

The speed of the arrest front is $v = (W_b - W_a)/n$, where n is the number of somites that are formed in the interval. (Developmental time is usually measured in units of number of somites.) The rate of somite formation is D_s/n. If the clock-and-wavefront model is true, then the rate of somite formation and the speed of the arrest front should be equal, so we should have $D_s = (W_b - W_a)$. This was tested in Gomez et al., *Nature*, **454**, 335–339, 2008, and the result is shown in Fig. 11. For each of four species, the ratio of the rate of arrest front movement to that of the formation of somites, $(W_b - W_a)/D_s$, is approximately unity, suggesting that the oscillation frequency is tuned with the front velocity, as given by the clock-and-wavefront model. However, note that this ratio is decidedly below unity for zebrafish.

The clock and wavefront model also makes valuable predictions about the size and number of somites in mutants. Consider first the ratio of the sizes of somites in wild type and mutant embryos. Here, we assume the mutations affect the genetic

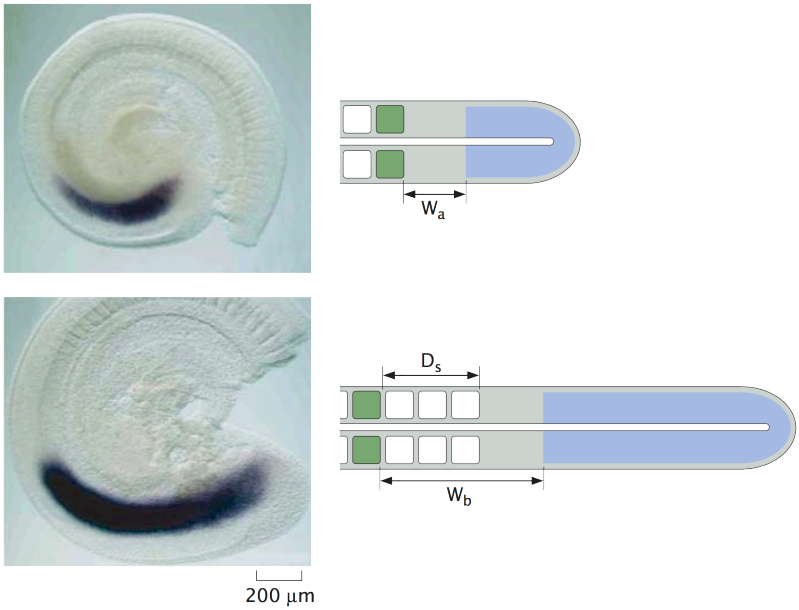

Figure 10: A schematic of a measurement of the arrest front speed and rate of somitogenesis in a corn snake embryo. The gene MSGN1 is stained to signify the location of the PSM. The arrest front is at the anterior edge of this stained region. The somites are also clearly visible. W_a and W_b are the positions of the arrest front at the beginning and end of a developmental time interval, and D_s is the length of somite region formed during the same time interval. From Phillips, et al., *Physical Biology of the Cell*, 2nd Ed., 2012, adapted from Gomez et al., *Nature*, **454**, 335–339, 2008.

oscillations and not the speed of the arrest front. Specifically, for the purposes of discussion, we will take $T_{\text{mut}} > T_{\text{wt}}$.

$$\frac{s_{\text{mut}}}{s_{\text{wt}}} = \frac{vT_{\text{mut}}}{vT_{\text{wt}}} = \frac{T_{\text{mut}}}{T_{\text{wt}}}. \tag{6.1}$$

So, we get larger somites with slower oscillations. Now, consider the ratio of the number of somites over the developmental time T_{dev}.

$$\frac{n_{\text{mut}}}{n_{\text{wt}}} = \frac{T_{\text{dev}}/T_{\text{mut}}}{T_{\text{dev}}/T_{\text{wt}}} = \frac{T_{\text{wt}}}{T_{\text{mut}}}, \tag{6.2}$$

which says that we get fewer somites.

6.3 PSM cells do not oscillate in unison

Despite some indirect experimental evidence supporting the original clock-and-wavefront model, such as in the Gomez et al. paper, direct observations of *her1* dynamics in the

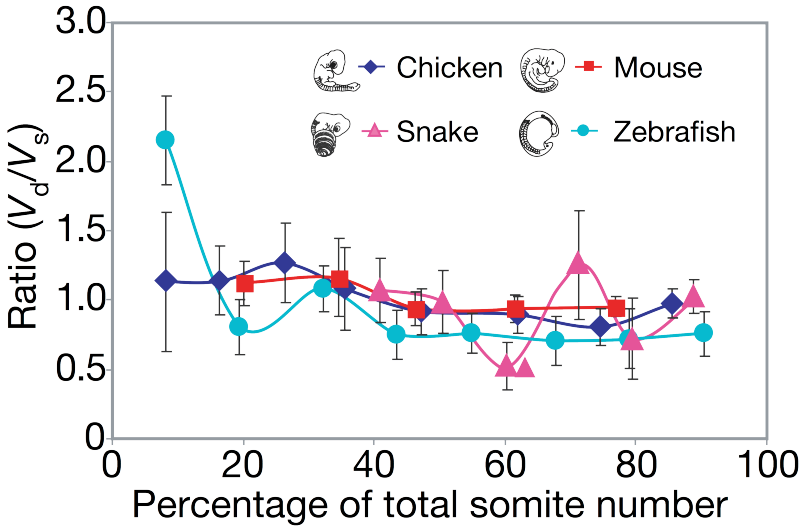

Figure 11: The ratio of the rate of the arrest front movement (V_d) to that of formation of somites (V_s). For all four species, this ratio is approximately unity. Adapted from Gomez et al., *Nature*, **454**, 335–339, 2008.

PSM show that the gene expression in the cells does not oscillate in unison. This was seen before by fixing and staining embryos at certain time point, but was more firmly demonstrated when Soroldoni, et al. (*Science*, **345**, 222–225, 2014) developed a reporter for *her1 in vivo*. As seen in Fig. 12, the expression of *her1* is not uniform. Further, we see that **kinematic waves** of *her1* expression travel toward the anterior where they are arrested.[6]

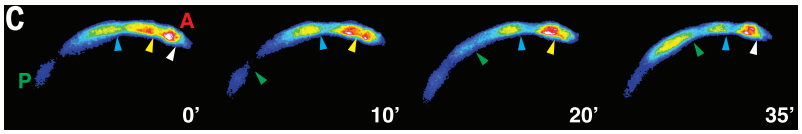

Figure 12: Image of *her1* expression over time in a developing zebrafish embryo. Waves of expression (each wave is identified and color coded with arrowheads) travel toward the posterior where they are arrested. Figure taked from Soroldoni, et al., *Science*, **345**, 222–225, 2014.

To understand how kinematic waves work, I borrow the analogy from the Soroldoni paper. Think about a stock ticker. Each light flicks on and off and there is some coupling to neighboring lights. The result is a movement of an image of lights across the ticker, even though each light bulb is stationary.

Since the observation of kinematic waves automatically eliminates the clock-and-wavefront hypothesis with a uniform oscillation frequency, we need to take a more

[6]This is better seen through a movie of this process, http://science.sciencemag.org/highwire/filestream/595541/field_highwire_adjunct_files/0/1253089s1.avi, though the link may not work for you because *Science* is a closed journal.

careful look at the oscillators.

6.4 Generic description of oscillatory gene expression in somitogenesis

To more generically describe somitogenesis, Soroldoni et al. describe the oscillations in the PSM generically as a function of space and time. To do this, we define a generic description of an oscillatory function. For any function $Q(x,t)$ that is oscillatory in time, we can write the dynamics at position x as

$$Q(x,t) = q_0 + q(x,t)\cos\phi(x,t), \tag{6.3}$$

where $\phi(x,t)$ is the **phase** of the oscillation, q_0 is the baseline, and $q(x,t)$ is the amplitude. The parameters q_0 and $q(x,t)$ capture the strength of the oscillatory signal, while the frequency information is captured in the phase. As an example, we get a pure cosine wave that is uniform in space if $\phi(x,t) = \omega t$, and a pure sine wave if $\phi(x,t) = \omega t - \pi/2$. The period of both of these waves is $T = 2\pi/\omega$.

Our analysis will focus on the phase of the oscillations, which is a result of the temporal dynamics of gene expression and coupling to neighboring cells. Let the x-position of the posterior end of the PSM be $x = 0$ and let $a(t)$ be the x-position of the anterior end of the PSM (the arrest front). We define $\phi_A = \phi(a(t),t)$ as the phase of the oscillators at the anterior and $\phi_P = \phi(0,t)$ as the phase of the oscillators at the posterior. Then, the number of kinematic waves, K, in the PSM is given by the total difference in phase, modulo 2π.

$$K = \frac{\phi_P - \phi_A}{2\pi} \tag{6.4}$$

Note that we do not wrap the phase shift here, i.e., $\phi = 2\pi$ is not the same as $\phi = 4\pi$.

To investigate how the number of kinematic waves changes in time, we compute the time derivative.

$$\frac{\mathrm{d}K}{\mathrm{d}t} = \frac{1}{2\pi}\left(\frac{\mathrm{d}\phi_P}{\mathrm{d}t} - \frac{\mathrm{d}\phi_A}{\mathrm{d}t}\right) = \frac{\omega_P - \omega_A}{2\pi} = \frac{1}{T_p} - \frac{1}{T_A}, \tag{6.5}$$

where we have defined

$$\omega = \frac{\partial\phi}{\partial t}. \tag{6.6}$$

This tells us that if the number of kinematic waves changes in time, then the period at the anterior is different than that at the posterior. This can be observed experimentally, and is one way of seeing a non-flat phase profile across the PSM.

I just used the word **phase profile** loosely to mean how the phase of the oscillators varies across the PSM. Let's codify that more concretely. We define the phase profile $\psi(x,t)$ as

$$\psi(x,t) = \phi(x,t) - \phi_P(t), \tag{6.7}$$

which is simply how the phase varies as we move away from the posterior. Then, we can write

$$\begin{aligned}\omega_A = \frac{\mathrm{d}\phi}{\mathrm{d}t} &= \frac{\mathrm{d}\phi_P}{\mathrm{d}t} + \frac{\mathrm{d}\psi(a(t),t)}{\mathrm{d}t} \\ &= \omega_P + \frac{\partial\psi(a(t),t)}{\partial t} + \frac{\mathrm{d}a}{\mathrm{d}t}\frac{\partial\psi(a(t),t)}{\partial x} \\ &= \omega_P + \omega_W + \omega_D,\end{aligned} \tag{6.8}$$

So, the difference in oscillation frequency between the anterior and posterior is $\omega_A - \omega_P = \omega_W + \omega_D$. We have defined $\omega_W \equiv \partial\psi(a(t),t)/\partial t$. This is the change in frequency that is inherent to the oscillators. Soroldoni, et al. call $2\pi/\omega_W$ the "dynamic wavelength," which gives the change of the wavelength of the kinematic waves in time. We have also defined

$$\omega_D = \frac{\mathrm{d}a}{\mathrm{d}t}\frac{\partial\psi(a(t),t)}{\partial x}. \tag{6.9}$$

This describes how the anterior phase differs from the posterior due to the Doppler effect. Since the PSM is shortening during development, the anterior is rushing into the kinematic waves, so the observed frequency is higher. Specifically, the speed of the observer is $\mathrm{d}a/\mathrm{d}t$ and the traveling wave has a wavelength of $2\pi(\partial\psi/\partial x)^{-1}$.

6.5 Assessment of models in terms of ω_A and ω_P

Soroldoni, et al. can measure the phase profile and can therefore deduce ω_D and ω_W. What do different models predict?

Clock-and-wavefront model. In this model, $\phi(x,t) = \omega t$, since all oscillators oscillate in unison with a constant frequency ω. Thus, $\phi(x,t) = \phi_P(t)\ \forall x$, so $\phi(x,t) = 0$. Thus, $\omega_D = \omega_W = 0$ and $\omega_A = \omega_P$.

Steady-state PSM. One might consider the scenario where the PSM is in steady state. That is to say that it does not grow or shrink, $a(t) = a_0$, and there is no modulation of the phase portrait, $\phi(x,t) = \omega t + \psi(x)$. In this case, ψ is not a function of time, so $\omega_W = 0$. The length of the PSM, a, is also not a function of time so, $\mathrm{d}a/\mathrm{d}t = 0$, meaning that $\omega_D = 0$. So, again, we have $\omega_A = \omega_P$ under this model.

Scaling wave pattern. In this model, the phase profile is a time-independent function of the *normalized* PSM length.

$$\phi(x,t) = \omega t + \psi(x/a(t)), \tag{6.10}$$

and we may have $\mathrm{d}a/\mathrm{d}t \neq 0$. Then, we have

$$\omega_W = \frac{\partial \psi(x/a(t))}{\partial t} = -\frac{1}{a}\frac{\mathrm{d}a}{\mathrm{d}t}\left.\frac{\partial \psi}{\partial (x/a(t))}\right|_{x/a(t)=1}, \tag{6.11}$$

and

$$\omega_D = \frac{\mathrm{d}a}{\mathrm{d}t}\frac{\partial \psi(x/a(t))}{\partial x} = \frac{1}{a}\frac{\mathrm{d}a}{\mathrm{d}t}\left.\frac{\partial \psi}{\partial (x/a(t))}\right|_{x/a(t)=1}, \tag{6.12}$$

So, in this case, ω_D and ω_W have equal magnitude and opposite sign. Thus, we again have $\omega_A = \omega_P$. Therefore, if we find experimentally that $\mathrm{d}K/\mathrm{d}t \neq 0$, we must have $T_P \neq T_A$, so therefore $\omega_P \neq \omega_A$, and none of these three models can be true.

7 Good talks: structuring your talk

Lecture 7 was on giving good talks; there are no lecture notes. The slides are available here.

8 Good talks: constructing good slides

Lecture 8 was on giving good talks; there are no lecture notes. The slides are available here.

9 Continuum mechanics I: conservation of mass

As we move into the mechanics of morphogenesis, we need to develop a mathematical framework, similar to our use of mass action kinetics in our studies of signaling. We have already seen some of the results of this analysis in our discussion of Turing patterns and the Ben-Zvi, et al. paper, where we already used some results pertaining to diffusive transport that we will soon derive. We will discuss this more formally now.

We will be working up to a hydrodynamic theory for active viscous nematic fluids, which we will use to model the actomyosin cortex in a developing *C. elegans* embryo. For a recent review of the theory of these types of complex materials, see this paper by Jülicher, Grill, and Salbreux.

9.1 Assumptions about continua

We will be treating cells and tissues as continua, meaning that we do not consider discrete molecules, or in some cases discrete cells. When is this a reasonable thing to do? When can we neglect molecular details?

We can think of an obvious example where it is ok to treat objects as continua. Let's say we are engineering a submarine. We want to design its shape and propeller such that it moves efficiently through water. Do we need to take into account the molecular details of the water? Definitely not! We only need to think about *bulk properties* of the water; its density and viscosity (both of which are temperature dependent). We can also define a velocity of water as a continuum as opposed to thinking about the trajectories of every molecule. So, clearly there are situations where the continuum treatment of a fluid is valid and in fact preferred.

Similarly, we do not need to know all of the details of the metal of the submarine. We would again need to know only bulk properties, such as its stiffness and thermal expansivity. We can also treat solids as continua.

There are also cases where we cannot use a continuum approximation. For example, if we are studying an aquaporin, we might want to analyze the electrostatic interactions as a single water molecule passes through. Clearly here we need to have a molecular/atomistic description of the system, at least of the water molecule itself.

So, when can we use a continuum description instead of a discrete one? We will have a more precise answer for this as we develop the theory in a moment, but for now, we'll just say that we need plenty of particles so that we can average their effects.

9.2 A preliminary: indicial notation

In order to more easily work our way through our treatment of continuum mechanics, we will introduce **indicial notation**, which is a convenient way to write down vectors, matrices and differential operators. This technique was invented by Albert Einstein.

Before plunging in, I note that we shouldn't trivialize or fear new notation. To quote Feynman, "We could, of course, use any notation we want; do not laugh at notations; invent them, they are powerful. In fact, mathematics is, to a large extent, invention of better notations."

The main concept behind indicial notation is a **tensor**. A tensor is a system of components organized by one or more indices that transform according to specific rules under a set of transformations. Tensors are parametrization-independent objects. The **rank** of a tensor is the number of indices it has. To help keep things straight in your mind, you can think of a tensor as a generalization of a scalar (rank 0 tensor), vector (rank 1 tensor) and a matrix (rank 2 tensor).[7] That's a mouthful, and quite abstract, so it's better to see how they behave with certain operations.

9.2.1 Contraction

The **contraction** of a tensor involves summing over like indices. For example, say we have two rank 1 tensors, a_i and b_i. Then, their contraction is

$$a_i b_i = a_1 b_1 + a_2 b_2 + \cdots . \tag{9.1}$$

It is convention in indicial notation to **always sum over like indices**. So, if a_i and b_i represent vectors in Cartesian three-space, which they usually will in our studies, they have components like (a_x, a_y, a_z). Then $a_i b_i = a_x b_x + a_y b_y + a_z b_z$ is the vector dot product. This relates to vector notation you might already be used to seeing.

$$a_i b_i = \mathbf{a} \cdot \mathbf{b}. \tag{9.2}$$

Note that in indicial notation, a_i represents the perhaps more familiar $\mathbf{a}$. Note also that the tensor operations we are defining are parametrization independent, and they need not, in general, represent Cartesian coordinates.

We have just seen that contraction of two rank one tensors gives a rank zero tensor. Similarly, we can contract a rank two tensor with a rank one tensor, which is equivalent to a matrix-vector dot product.

$$A_{ij} b_j = c_i. \tag{9.3}$$

[7] We will not talk about covariant and contravariant tensors in this class, since they are not necessary for what we are studying.

Since we summed (or contracted) over the index j, the index i remains. It is helpful to write it out for the case of $i, j \in \{x, y, z\}$.

$$A_{ij} = \begin{pmatrix} A_{xx} & A_{xy} & A_{xz} \\ A_{yx} & A_{yy} & A_{yz} \\ A_{zx} & A_{zy} & A_{zz} \end{pmatrix}, \tag{9.4}$$

and $b_j = (b_x, b_y, b_z)$. Then, we have

$$c_i = A_{ij} b_j = \begin{pmatrix} A_{xx}b_x + A_{xy}b_y + A_{xz}b_z \\ A_{yx}b_x + A_{yy}b_y + A_{yz}b_z \\ A_{zx}b_x + A_{zy}b_y + A_{zz}b_z \end{pmatrix}. \tag{9.5}$$

This is equivalent to $\mathsf{A} \cdot \mathbf{b}$ in notation you may be more accustomed to. Note that $A_{ij}b_i$ is equivalent to $\mathsf{A}^\mathsf{T} \cdot \mathbf{b}$. Stated explicitly, with indicial notation on the left hand side and vector notation on the right hand side,

$$\text{entry } i \text{ of } A_{ij}b_j = (\mathsf{A} \cdot \mathbf{b})_i, \tag{9.6}$$

$$\text{entry } j \text{ of } A_{ij}b_i = (\mathsf{A}^\mathsf{T} \cdot \mathbf{b})_j. \tag{9.7}$$

9.2.2 Direct product

We can also make higher order tensors from lower order ones. For example, $a_i b_j$ gives a second order tensor.

$$a_i b_j = \begin{pmatrix} a_x b_x & a_x b_y & a_x b_z \\ a_y b_x & a_y b_y & a_y b_z \\ a_z b_x & a_z b_y & a_z b_z \end{pmatrix}. \tag{9.8}$$

Comparing to vector notation, entry i, j of $a_i b_j = (\mathbf{a} \otimes \mathbf{b})_{ij}$.

9.2.3 Differential operations

You have probably seen the gradient operator before. In Cartesian coordinates, it is

$$\nabla = \left(\frac{\partial}{\partial x}, \frac{\partial}{\partial y}, \frac{\partial}{\partial z} \right). \tag{9.9}$$

In indicial notation, this is ∂_i. So, the gradient of a scalar function f is $\partial_i f$, which is a rank 1 tensor, as we would expect. In perhaps more familiar notation, we would write this as ∇f. The divergence of a vector v_i, commonly written as $\nabla \cdot \mathbf{v}$, is $\partial_i v_i$. This is a contraction of the differential operator with the vector. The Laplacian of a scalar, commonly written as $\nabla^2 f$ or Δf, is $\partial_i \partial_i f$.

9.2.4 Trace and matrix multiplication

We can define the trace of a rank 2 tensor as the sum of the diagonal elements.

$$A_{ii} = A_{xx} + A_{yy} + A_{zz}. \tag{9.10}$$

Note that we could multiply matrices and then take the trace. Comparing to familiar notation,

$$A_{ij}B_{ij} = \mathrm{tr}(\mathsf{A}^{\mathsf{T}} \cdot \mathsf{B}). \tag{9.11}$$

In other words, the contracted indices tell us what to sum. Simple matrix multiplication is

$$A_{ij}B_{jk} = (\mathsf{A} \cdot \mathsf{B})_{ik}. \tag{9.12}$$

9.2.5 The Levi-Civita symbol

We represent cross products with the **Levi-Civita symbol**. This is defined as

$$\varepsilon_{ijk} = \begin{cases} 1 & \text{if } ijk = xyz, yzx, zxy \\ -1 & \text{if } ijk = zyx, yxz, xzy \\ 0 & \text{otherwise.} \end{cases} \tag{9.13}$$

Thus, we can represent the vector cross product as

$$\text{entry } i \text{ in } \varepsilon_{ijk}u_j v_k = (\mathbf{u} \times \mathbf{v})_i. \tag{9.14}$$

The curl of a vector field is

$$\text{entry } k \text{ in } \varepsilon_{ijk}\partial_i v_j = (\nabla \times \mathbf{v})_k = (\mathrm{curl}\,\mathbf{v})_k. \tag{9.15}$$

9.3 Conservation of mass

Now that we have the mathematical notation in place, we will proceed to derive conservation laws for a continuous material. To do this, consider a piece of space within a material, which we will call a **volume element**. The volume element has an outward normal vector n_i, as shown in Fig. 13.

Now, let's say that this volume element has material in it with a density ρ. Then, the total mass of material inside the volume element is

$$m = \int \mathrm{d}V\, \rho\,, \tag{9.16}$$

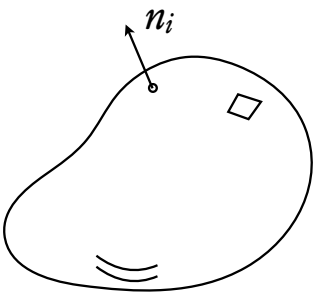

Figure 13: Drawing of a three-dimensional volume element with outward normal n_i.

where the integral is over the volume. Now, the time rate of change of mass in the volume must be equal to the net flow of mass into the control volume. The mass flow rate *out* of control volume per unit area is $n_i(\rho v_i)$, where v_i is the velocity of material. So, the rate of change of mass is

$$\partial_t \int \mathrm{d}V\, \rho = -\int \mathrm{d}S\, n_i(\rho v_i), \tag{9.17}$$

where the second integral is over the surface of the control volume.

We will now make use of the **divergence theorem**, also known as Gauss's theorem or the Gauss divergence theorem, which states that for any closed surface, any continuously differentiable tensor field F_i satisfies

$$\int \mathrm{d}V\, \partial_i F_i = \int \mathrm{d}S\, n_i F_i. \tag{9.18}$$

This generalizes for higher rank tensor fields. E.g.,

$$\int \mathrm{d}V\, \partial_j T_{ij} = \int \mathrm{d}S\, n_j T_{ij}, \tag{9.19}$$

for a rank 2 tensor. Taking our tensor field as ρv_i, we apply the divergence theorem to get

$$\partial_t \int \mathrm{d}V\, \rho = -\int \mathrm{d}V\, \partial_i(\rho v_i). \tag{9.20}$$

We can take the time derivative inside the integral sign and rearrange to get

$$\int \mathrm{d}V\, (\partial_t \rho + \partial_i(\rho v_i)) = 0. \tag{9.21}$$

This must be true for all arbitrary control volumes, which means that the integrand must be zero, or

$$\partial_t \rho + \partial_i(\rho v_i) = 0. \tag{9.22}$$

We define the operator

$$\frac{\mathrm{d}}{\mathrm{d}t} \equiv \partial_t + v_i \partial_i \tag{9.23}$$

as the **material derivative** (also known as the substantial derivative), which is the time derivative in the **co-moving frame**. The second term in its definition in effect puts the observer moving along with this control volume in the material. Using the definition of the material derivative and the chain rule, we have

$$\frac{\mathrm{d}\rho}{\mathrm{d}t} = -\rho\, \partial_i v_i. \tag{9.24}$$

If ρ does not change, i.e., if the material is **incompressible**, the result is that the velocity field is divergenceless (also called solenoidal), or

$$\partial_i v_i = 0. \tag{9.25}$$

This result is called the **continuity equation**.

9.4 Conservation of mass for each species

The same analysis applies for the conservation of mass for a given species k. We will write k as a superscript with the understanding that repeated superscript indices are *not* implicitly summed over (though we may explicitly sum over them if we like). We start with the analog of equation (9.17). We define ρ^k as the density of species k and v_i^k as the velocity of particles of type k, and we have

$$\int \mathrm{d}V\, \partial_t \rho^k = -\int \mathrm{d}S\, n_i (\rho^k v_i^k) + \text{net production of } k \text{ by chemical reaction}. \tag{9.26}$$

I have added the production of k by chemical reaction (in words) to this equation, since we need to consider this as well. We can write this using the stoichiometric coefficients for chemical reaction l, ν_l^k, and their respective rates, r_l.

$$\int \mathrm{d}V\, \partial_t \rho^k = -\int \mathrm{d}S\, n_i (\rho^k v_i^k) + \int \mathrm{d}V\, M^k \nu_l^k\, r_l, \tag{9.27}$$

where M^k is the molar mass of species k. The expressions for r_l are typically given by mass action expressions. Now, we can apply the divergence theorem and rearrange, giving

$$\partial_t \rho^k = -\partial_i (\rho^k v_i^k) + M^k \nu_l^k\, r_l. \tag{9.28}$$

To both sides of this equation, we add $\partial_i(\rho^k v_i)$. The result is

$$\partial_t \rho^k + \partial_i(\rho^k v_i) = \frac{\mathrm{d}\rho^k}{\mathrm{d}t} + \rho^k \partial_i v_i = -\partial_i(\rho^k(v_i^k - v_i)) + M^k \nu_l^k r_l. \tag{9.29}$$

We define the **diffusive mass flux** by $j_i^k = \rho^k(v_i^k - v_i)$. This is the relative movement of species k compared to the center of mass, or **barycentric** movement. So we have

$$\frac{\mathrm{d}\rho^k}{\mathrm{d}t} = -\rho^k \partial_i v_i - \partial_i j_i^k + M^k \nu_l^k r_l. \tag{9.30}$$

We can re-write this equation in terms of the number density (the concentration) of species k instead of the mass density. It is as simple as dividing the entire equation by the molar mass.

$$\frac{\mathrm{d}c^k}{\mathrm{d}t} = -c^k \partial_i v_i - \frac{1}{M^k} \partial_i j_i^k + \nu_l^k r_l. \tag{9.31}$$

It is common to also use the symbol j_l^k for the **diffusive particle flux**, which is the diffusive mass flux divided by the molar mass. This double notation can be confusing, and we will avoid using it here.

Deriving an expression for the diffusive particle flux is nontrivial[8], and we will not do it here. We will take as given **Fick's first law**, which states that

$$\frac{j_i^k}{M^k} = -D^k \partial_i c^k, \tag{9.32}$$

where D^k is the (strictly positive) diffusion coefficient of species k. Using this expression, we arrive at the **reaction-diffusion-advection** equation,

$$\partial_t c^k = -\partial_i(c^k v_i) + \partial_i(D^k \partial_i c^k) + \nu_l^k r_l. \tag{9.33}$$

The diffusion coefficient is often constant (though not always, especially in developmental systems when phosphorylation states can alter the effective diffusion coefficient), so we get

$$\partial_t c^k = -\partial_i(c^k v_i) + D^k \partial_i \partial_i c^k + \nu_l^k r_l. \tag{9.34}$$

The first term on the right hand side describes the change in concentration as a result of being embedded in a moving material (advection). The second term describes diffusion, and the last describes chemical reaction. These are the same equations that we encountered in studying Turing patterns, sans the advective term. We see now that the equation is derived simply by accounting for all of the mass in an arbitrary volume element.

[8]It involves invoking the Second Law of Thermodynamics and some symmetry arguments. Importantly, it requires little else, and arrives naturally without substantial assumptions.

9.5 Shoring up when we can use continua

From the above, we can see what the criteria are for using continuum mechanics. We have to be able to define volume elements large enough to contain enough particles such that each volume element has a well defined average and does not experience large fluctuations. The volume elements must be small enough that we can define spatial derivatives of these average quantities. So, we need to have a system big enough and full enough to contain many sufficiently big volume elements. This seems restrictive, but in practice, continuum mechanics has been very successful even in describing phenomena on very small length scales.

9.6 General conservation law

Instead of counting mass, let's count any other conserved quantity that is a property of the material; let's call it ξ. If j_i is the flux of ξ out of the volume element Then, we have

$$\partial_t \int \mathrm{d}V\, \xi = -\int \mathrm{d}S\, n_i j_i, \tag{9.35}$$

or, upon applying the divergence theorem and considering that the volume element is arbitrary,

$$\partial_t\, \xi = -\partial_i j_i. \tag{9.36}$$

This tells us that the local time rate of change of a conserved quantity is given by the divergence of a flux, an important general result.

10 Continuum mechanics II: conservation of momentum

10.1 Conservation of linear momentum

Recall the general conservation law,

$$\partial_t \xi = -\partial_i j_i. \tag{10.1}$$

Let's take $\xi = \rho v_i$, the linear momentum density. The total linear momentum of a volume element is $\int \mathrm{d}V \rho v_i$, so taking $\xi = \rho v_i$ means that we are describing a conservation law for linear momentum. In this case, $\partial_t(\rho v_i)$ is a rank one tensor, so the flux must be a rank two tensor. We will denote this flux as Σ_{ij}, the **total momentum flux tensor**. It is the flux of momentum density coming out of a volume element. The statement of conservation of linear momentum, called the equation of motion, is

$$\partial_t \rho v_i = -\partial_j \Sigma_{ij}. \tag{10.2}$$

We can split the total momentum flux tensor into two pieces. First, we have the momentum flux due to material flowing in and out of the volume element. This is $\rho v_i v_j$. The second part of the total momentum flux is all the other stuff, which we will denote by σ_{ij}. This object, σ_{ij}, is called the **stress tensor**.

$$\Sigma_{ij} = \rho v_i v_j + \sigma_{ij}. \tag{10.3}$$

To be clear, the stress tensor contains all stresses suffered by a material, such as pressure and shear stresses. The other part of the total momentum flux tensor is momentum density that is transported by virtue of material moving in and out of the volume element. Using this split total momentum tensor, we have

$$\partial_t \rho v_i = -\partial_j \rho v_i v_j - \partial_j \sigma_{ij}. \tag{10.4}$$

Applying the chain rule to terms on both sides of this equation gives

$$\rho \partial_t v_i + v_i \partial_t \rho = -\rho v_j \partial_j v_i - v_i \partial_j \rho v_j - \partial_j \sigma_{ij}. \tag{10.5}$$

Rearranging, we get

$$\rho (\partial_t + v_j \partial_j) v_i = -v_i [\partial_t \rho + \partial_j \rho v_j] - \partial_j \sigma_{ij}. \tag{10.6}$$

The parenthetical term on the left hand side is the material derivative. The bracketed term is zero by conservation of mass, cf. equation (9.22). Thus, we arrive at our statement of conservation of linear momentum.

$$\rho \frac{\mathrm{d}v_i}{\mathrm{d}t} = -\partial_j \sigma_{ij}. \tag{10.7}$$

10.2 Physical interpretation of the stress tensor

The stress tensor describes forces resulting from relative motion of a material. It has units of force per area, or momentum flux. To see this, note that momentum has dimension of ML/T. A flux introduces dimension of $1/L^2T$. Putting it together, the stress has units of M/LT^2, or force per area.

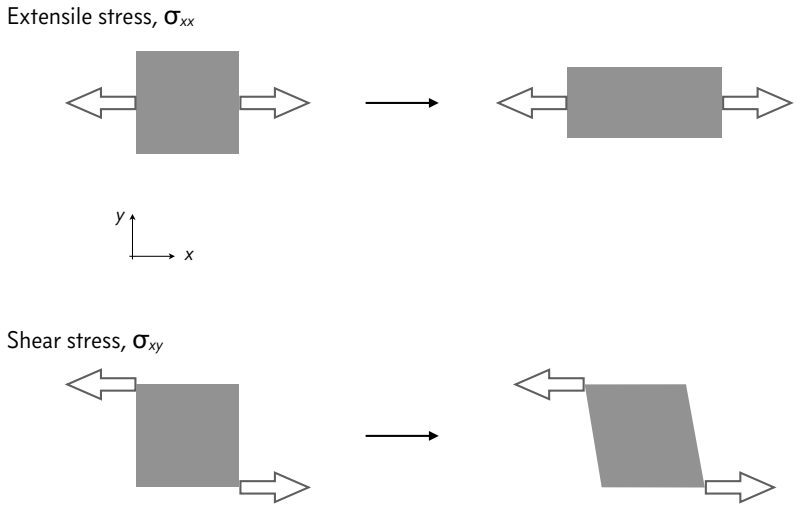

Figure 14: Depiction of extensile and shear stresses on a block of material.

To understand how it describes forces due to relative motion consider grabbing a piece of material and stretching it, as in the top illustration in Fig. 14. The part of the material to the left moves leftward and that to the right moves rightward. The component of the stress tensor describing resistance to this mode of relative motion is σ_{xx}.

Now consider a shearing motion, as in the bottom illustration in Fig. 14. The component of the stress tensor describing resistance to this mode of relative motion is σ_{xy}.

10.3 Constitutive relations

This is all fine and good, but can we write a mathematical expression for σ_{ij} so that we can put it to use? An expression for the stress tensor is called a **constitutive relation**. A constitutive relation relates physical quantities in a material-specific way. We already saw a constitutive relation in the last lecture, Fick's first law, which relates diffusive mass flux to a concentration gradient, $j_i^k = -M^k D^k \partial_i c^k$.

We stated Fick's first law without proof, and the derivations constitutive relations are often nontrivial. We will explore constitutive relations in the this and the next lecture and explore their meanings.

10.4 Constitutive relation for a homogeneous elastic solid

We first consider a homogeneous elastic solid. The stress tensor is given in terms in the **strain** tensor, which we will first characterize. Throughout the following discussion, bear in mind that we are talking about a *homogeneous* solid. This means that deforming the solid in the x-direction should be the same as deforming it in the y-direction.

10.4.1 Elastic strain tensor

We define by x_i the position of a piece of the solid in space. We then deform the solid such that that same piece is now at position x_i'. We define the **displacement**, $u_i = x_i' - x_i$. If u_i is constant across the solid, the solid is not being deformed; rather, it is being translated in the direction of u_i. However, if u_i varies in space, we do have a deformation. So, the quantity $\partial_i u_j$ reflects local deformations in the solid.

To investigate the magnitude of deformations, we consider the differential squared distance between neighboring points in the solid.

$$\mathrm{d}\ell^2 = \mathrm{d}x_i\,\mathrm{d}x_i. \tag{10.8}$$

If we have a deformation, this distance changes by

$$\mathrm{d}\ell'^2 = \mathrm{d}x_i'\,\mathrm{d}x_i'. \tag{10.9}$$

To get an expression for $\mathrm{d}x_i'$, we can use the chain rule.

$$\mathrm{d}(x_i' - x_i) = \mathrm{d}u_i = (\partial_j u_i)\mathrm{d}x_j, \tag{10.10}$$

which gives

$$\mathrm{d}x_i' = \mathrm{d}x_i + (\partial_j u_i)\mathrm{d}x_j. \tag{10.11}$$

Then, we have

$$\begin{aligned}
\mathrm{d}\ell'^2 &= (\mathrm{d}x_i + (\partial_j u_i)\mathrm{d}x_j)\,(\mathrm{d}x_i + (\partial_k u_i)\mathrm{d}x_k) \\
&= \mathrm{d}x_i\,\mathrm{d}x_i + (\partial_j u_i)\mathrm{d}x_j\,\mathrm{d}x_i + (\partial_k u_i)\mathrm{d}x_k\,\mathrm{d}x_i + (\partial_j u_i)(\partial_k u_i)\mathrm{d}x_j\,\mathrm{d}x_k \\
&= \mathrm{d}\ell^2 + [\partial_i u_j + \partial_j u_i + (\partial_i u_k)(\partial_j u_k)]\,\mathrm{d}x_i\,\mathrm{d}x_j,
\end{aligned} \tag{10.12}$$

where in the last line we have renamed indices to collect terms multiplying $\mathrm{d}x_i\,\mathrm{d}x_j$. We can write this down as

$$\mathrm{d}\ell'^2 - \mathrm{d}\ell^2 = 2\,\varepsilon_{ij}\,\mathrm{d}x_i\,\mathrm{d}x_j, \tag{10.13}$$

where we have defined the **strain tensor**[9] as

$$\varepsilon_{ij} = \frac{1}{2}\left(\partial_i u_j + \partial_j u_i + (\partial_i u_k)(\partial_j u_k)\right). \tag{10.14}$$

Because it goes as the square of the differential displacement, the last term in the strain tensor is small for small displacements. So we have, to linear order in $\partial_i u_i$,

$$\varepsilon_{ij} \approx \frac{1}{2}(\partial_i u_j + \partial_j u_i). \tag{10.15}$$

10.4.2 Elastic stress tensor

We have established that the strain describes deformations of the solid. We can derive a relationship between the stress tensor, which describes the forces necessary to achieve the deformations, and the strain tensor using thermodynamic arguments. Instead, we will just start with Hooke's law, which is valid for small deformations. As Hooke said, "*ut tensio sic vis*," or the force is proportional to extension. Because the stress tensor is a rank 2 tensor, as is the strain tensor, to write a linear relationship between the two, most generally, we need a rank 4 tensor.

$$\sigma_{ij} = C_{ijkl}\,\varepsilon_{kl}. \tag{10.16}$$

There are $3^4 = 81$ entries in the tensor C_{ijkl}. This looks really intimidating, but by symmetry arguments, we can show that the entries are not all independent. For example, because the strain tensor ε_{ij} is symmetric, $\varepsilon_{ij} = \varepsilon_{ji}$. The stress tensor must also show this symmetry, so therefore so must C_{ijkl}. This implies that $C_{ijkl} = C_{jikl} = C_{ijlk}$. We will not go through all of the symmetry arguments here, but in the end, we find that there are only two independent parameters. Generally, it can be shown that a linear relationship between two rank 2 symmetric tensors that remains invariant under change of coordinates has the form

$$\sigma_{ij} = \lambda\,\varepsilon_{kk}\,\delta_{ij} + 2\mu\,\varepsilon_{ij}, \tag{10.17}$$

where the constants λ and μ are called the **Lamé coefficients**. This gives us our constitutive relation for an elastic solid.

As is commonly done, is is convenient to write the Lamé coefficients in a different form. We define

$$\lambda = \frac{E\nu}{(1+\nu)(1-2\nu)}, \tag{10.18}$$

$$\mu = \frac{E}{2(1+\nu)}, \tag{10.19}$$

[9] Though they have similar symbols, this strain tensor ε_{ij} is not to be confused with the Levi-Civita symbol ε_{ijk}.

where E is called the Young's modulus and ν is the Poisson ratio.[10] The resulting expression for the stress tensor is

$$\sigma_{ij} = \frac{E}{1+\nu}\left(\varepsilon_{ij} + \frac{\nu}{1-2\nu}\,\varepsilon_{kk}\,\delta_{ij}\right), \tag{10.20}$$

We will not derive it here, but the second law of thermodynamics dictates that $E \geq 0$ and $-1 \leq \nu \leq 1/2$. Thus, the stress associated with an elastic deformation is of order $E\varepsilon$.

10.4.3 Equation of motion for an elastic solid

Now that we have our constitutive relation, we can write the equation of motion from the statement of conservation of linear momentum. The local velocity, v_i, is related to the displacement as $v_i = \partial_t u_i$. Thus, we can write

$$\rho\,\frac{\mathrm{d}v_i}{\mathrm{d}t} = \rho\,\left(\partial_t^2 u_i + (\partial_t u_j)\partial_j \partial_t u_i\right) = -\partial_j \sigma_{ij}, \tag{10.21}$$

where the t's denote time derivatives and are not summed over. Evidently, this is a wave equation in the displacement. The dynamics describe elastic waves through the solid. We know these waves as sound. The dynamics are usually very fast compared to biological time scales of interest, so we usually neglect the left hand side of the equation of motion. Typically with elastic solids, we will study only statics, as governed by the constitutive relation itself, in this case, equation (10.20).

10.5 Constitutive relation for an isotropic viscous fluid

If we look at the expression for the elastic stress, we see that it scales like the displacement, $\sigma \sim E\varepsilon$. For a fluid, we would not expect this to be the case. If we displace a fluid and then let it rest, we do not have to exert any more force to maintain the displacement. Instead, we expect that the stress we need to exert on a fluid to move it will be related to the *rate* at which we make deformations,

$$\partial_t \partial_i u_j = \partial_i \partial_t u_j = \partial_i v_j, \tag{10.22}$$

where $v_j = \partial_t u_j$ is the velocity at which the material is moving. In other words, if we want to move a fluid more rapidly, it will require more force than to move it slowly. The actual magnitude of the displacement will not matter; only the rate at which we make displacements. The **velocity gradient tensor** can be written as

$$\partial_i v_j = \frac{1}{2}(\partial_i v_j + \partial_j v_i) + \frac{1}{2}(\partial_i v_j - \partial_j v_i) = v_{ij} + \omega_{ij}. \tag{10.23}$$

[10] There should be no confusion between the Poisson ration ν and the stoichiometric coefficient for species k in chemical reaction l, ν_{il}^k.

Here, we have defined

$$v_{ij} \equiv \frac{1}{2}(\partial_i v_j + \partial_j v_i) \tag{10.24}$$

as the symmetric part of the velocity gradient tensor and

$$\omega_{ij} \equiv \frac{1}{2}(\partial_i v_j - \partial_j v_i) \tag{10.25}$$

as the antisymmetric part. Due to the symmetry of an isotropic fluid and conservation of angular momentum (which we will not formally consider here), the stress tensor must be symmetric, which means that ω_{ij} does not contribute to it.

We might also expect the stress to include the hydrostatic pressure, p. After all, pumps move fluids around by exerting pressure on them. So, we additionally have a $-p\,\delta_{ij}$ term in the stress tensor. For an isotropic viscous fluid, then, we have

$$\sigma_{ij} = -p\,\delta_{ij} + C_{ijkl} v_{kl}. \tag{10.26}$$

Again, we use the fact that a linear relationship between two rank 2 symmetric tensors that remains invariant under change of coordinates can be written with Lamé coefficients.

$$\sigma_{ij} = -p\,\delta_{ij} + \lambda\, v_{kk}\,\delta_{ij} + 2\mu\, v_{ij}. \tag{10.27}$$

We will define η and η_v such that $\mu = \eta$ and $\lambda = (\eta_v - 2\eta)/3$. Then, we have

$$\sigma_{ij} = -p\,\delta_{ij} + 2\eta\left(v_{ij} - \frac{v_{kk}}{3}\,\delta_{ij}\right) + \frac{\eta_v}{3}\, v_{kk}\,\delta_{ij}. \tag{10.28}$$

The quantity η is called the **viscosity**, or shear viscosity, and η_v is called the bulk viscosity. It is clear that η_v determines the contribution of isotropic compression to the stress. For am incompressible fluid, the continuity equation (9.25) gives that $v_{kk} = \partial_k v_k = 0$, so the stress tensor is

$$\sigma_{ij} = -p\,\delta_{ij} + 2\eta\, v_{ij} = -p\,\delta_{ij} + \eta\,(\partial_i v_j + \partial_j v_i). \tag{10.29}$$

10.6 Equation of motion for an incompressible isotropic viscous fluid

Now that we have the constitutive relation, we can write down the equation of motion for an incompressible isotropic viscous fluid. This is the statement of conservation of linear momentum.

$$\frac{\mathrm{d}v_i}{\mathrm{d}t} = -\partial_j \sigma_{ij} = \partial_i p - \eta\,\partial_j\partial_j v_i, \tag{10.30}$$

This equation, together with the continuity equation, $\partial_i v_i = 0$, are known as the **Navier-Stokes equations**. We can nondimensionalize this equation, choosing $x = \ell\tilde{x}$, $t = \tau\tilde{t}$, $v_i = U\tilde{v}_i$, and $p = \tilde{p}\,\eta\,U/\ell$. Here, ℓ and τ are respectively length and time scales of interest, and U is the characteristic velocity. The resulting equation is

$$\frac{\rho\,\ell^2}{\eta\tau}\,\partial_t\tilde{v}_i + \frac{\rho U\ell}{\eta}\,\tilde{v}_j\partial_j\tilde{v}_j = \partial_i\tilde{p} - \partial_j\partial_j\tilde{v}_i, \tag{10.31}$$

where the derivatives are now with respect to dimensionless variables. We can collect the constants to define dimensionless parameters, the **Reynolds number**, $\mathrm{Re} = \rho U\ell/\eta$, and the **Strouhal number**, $\mathrm{Sr} = (\ell/U)/\tau$.

$$\mathrm{Re}\,(\mathrm{Sr}\,\partial_t + \partial_j\tilde{v}_j)\,\tilde{v}_i = \partial_i\tilde{p} - \partial_j\partial_j\tilde{v}_i. \tag{10.32}$$

The Reynolds number is the ratio of the inertial energy, $\rho U^2\ell^3$, to the energy loss due to viscous dissipation, $\eta U\ell^2$. The Strouhal number is the ratio of the advective time scale, ℓ/U to any other pertinent time scale of interest, τ. If $\mathrm{Re} \ll 1$ and $\mathrm{Re}\,\mathrm{Sr} \ll 1$, then the left hand side of the equation of motion is negligible compared to each term in the right hand side. In cell and developmental biology, this is generally the case. To satisfy us that this is indeed the case, we can estimate the Reynolds number for processes in a developing embryo. The density of our material is close to that of water, or 10^3 kg/m^3. The smallest viscosity is that of water, which is about 10^{-3} kg-m/s. The longest length scale we generally consider in early embryos is about 1 mm = 10^{-3} m. The fastest speeds could conceivably be that of the fastest motor proteins, about 100 μm/s = 10^{-4} μm/s. Putting this together gives a Reynolds number of $\mathrm{Re} = 0.1$. We have intentionally vastly overestimated this, since most fluid-like embryonic movements much more slowly, over shorter distances, and with much higher viscosity. So, we are generally justified in neglecting the left hand side of the equation of motion, and we have

$$\partial_j\sigma_{ij} = 0. \tag{10.33}$$

We will talk in more depth about dynamics of isotropic incompressible viscous fluids at low Reynolds number when we study the He, at al. paper. In a future lecture, we will look at complex fluid (those that are not isotropic, such as an actin cortex, which is comprised of filaments) and *active*, meaning that the material can consume energy (for example via ATP hydrolysis by motor proteins), which will use in the papers we read about polarizing the one-cell *C. elegans* embryo.

11 Viscous flows in development

In the He, et al. paper, we will study viscous flows in the context of apical constriction in ventral furrow formation in *Drosophila* development. He and coworkers do not consider the contracting material, but rather the passive components beneath. These can be modeled as a viscous fluid.

11.1 Dynamical equations of Stokes flow

An isotropic viscous fluid has a stress tensor given by

$$\sigma_{ij} = -p\,\delta_{ij} + 2\eta\, v_{ij} = -p\,\delta_{ij} + \eta\,(\partial_i v_j + \partial_j v_i). \tag{11.1}$$

The equation of motion, as we have seen before is

$$\rho\,\frac{\mathrm{d}v_i}{\mathrm{d}t} = \partial_j \sigma_{ij}, \tag{11.2}$$

where $\mathrm{d}/\mathrm{d}t$ denotes the material derivative we have seen in previous lectures. In most developmental contexts, the Reynolds number is very small, so the left hand side of the equation of motion is effectively zero. The resulting equation of motion is then

$$\partial_j \sigma_{ij} = -\partial_i p + \eta\,\partial_j\partial_j v_i = 0. \tag{11.3}$$

We have used the continuity equation, $\partial_i v_i = 0$, in writing this, and have made the assumption that the viscosity η is constant. Flow described by these equations is called **Stokes flow**, named after George Stokes, who was a pioneer in the study of low Reynolds number fluid dynamics.

11.2 Qualitative features of Stokes flow

Now that we have the equations governing Stokes flow, we can make some very powerful qualitative statements about Stokes flow.

1. The Stokes equations are linear. Therefore, for a given set of boundary conditions, the velocity field is unique. This is not true for flows with $\mathrm{Re} > 0$.
2. There is no time present in the Stokes equations, except possibly for time-dependent boundary conditions. This means that the flow field is set *instantaneously* by the boundary conditions. Knowledge of the flow at any other time is unnecessary.

3. Because the Stokes equations are linear, the dynamics are **reversible**. This means that if v_i is a solution of the Stokes equations, then so is $-v_i$ if the sign of the pressure field is also flipped.

$$-\partial_i(-p) + \eta\,\partial_j\partial_j(-v_i) = \partial_i p - \eta\,\partial_j\partial_j v_i = 0 = -\left(-\partial_i p + \eta\,\partial_j\partial_j v_i\right). \tag{11.4}$$

This also means that the dynamics are reversible in time. That is, if the time-dependent boundary conditions were run in reverse, the fluid dynamics would be exactly reversed as well.

4. Hydrodynamic forces are long-ranged. To see this, consider an object moving through a fluid. The fluid around the object moves, and as a result, momentum is carried through the fluid. The momentum flux is given by the stress tensor. So,

$$\text{momentum flux} \equiv j_{\text{mom}} \sim \partial_j v_i \sim \partial_r v, \tag{11.5}$$

where r is the radial distance from the translating object. We will assume a power law dependence of the momentum flux on r,

$$j_{\text{mom}} \sim r^{-\alpha-1}. \tag{11.6}$$

The total momentum flux through any spherical shell of radius R must be the same as any other spherical shell. The total momentum flux through a spherical shell scales like $j_{\text{mom}}R^2 \sim R^{-\alpha+1}$. For this to be the same for all shells, we must have $\alpha = 1$. Thus,

$$\partial_r v \sim r^{-2}, \tag{11.7}$$

such that $v \sim r^{-1}$. So, the velocity field decays away like $1/r$, in contrast to high Reynolds number where it decays away like $1/r^3$. In two dimensions, the decay is even slower, $v \sim \ln r$. So, hydrodynamic forces are felt over large distances.

11.3 Green's functions for Stokes flow

Consider a point force F_i in a fluid. In this case, the governing equations are

$$-\partial_i p + \eta\,\partial_j\partial_j v_i = -F_i\,\delta(x_i), \tag{11.8}$$

$$\partial_i v_i = 0. \tag{11.9}$$

The velocity and pressure fields that solve these equations are known as the **Green's functions**. We could solve for the Green's functions, but it is perhaps easier to "invent" the solution and then verify that it works. The result is

$$v_i = \frac{1}{8\pi\eta}\,F_j G_{ij}, \tag{11.10}$$

$$p = \frac{1}{8\pi\eta} F_i P_i, \tag{11.11}$$

where

$$G_{ij} = \frac{\delta_{ij}}{r} + \frac{x_i x_j}{r^3}, \tag{11.12}$$

$$P_i = 2\eta \frac{x_i}{r^3} + P_i^{\infty}, \tag{11.13}$$

where $r = \sqrt{x_i x_i}$ and $F_i P_i^{\infty}$ is the pressure very far away from the point source. From this expression, we see the $1/r$ dependence of the velocity field. Here, G_{ij} is known as the **Oseen tensor**, after the Swedish physicist Carl Wilhelm Oseen. The quantity v_i, as defined above, is the Green's function for the Stokes equations, is called a **Stokeslet**. The stress field from the point source is $F_k \Sigma_{ijk}$, where

$$\Sigma_{ijk} = -\frac{3}{4\pi} \frac{x_i x_j x_k}{r^5}. \tag{11.14}$$

In two dimensions, velocity field is instead

$$v_i = \frac{1}{4\pi\eta} F_j G_{ij}, \tag{11.15}$$

$$G_{ij} = \ln r \delta_{ij} - \frac{x_i x_j}{r^2}, \tag{11.16}$$

so the decay of the velocity field is even slower than in three dimensions.

11.4 Solutions of Stokes equations using Green's functions

He, et al. solved the Stokes equations by choosing a distribution and strength of point forces such that the fluid flow velocity matched that what was measured at he apical surface. In other words, the apical surface is contracting and constitutes a moving boundary. The boundary conditions were approximated by placing point sources that gave the right result at the boundary. Because the solution to the Stokes equations is unique, this gives the correct fluid flow. Note, however, that this crude method does not give the correct stresses. Getting those requires more careful methods like boundary integral methods, which are beyond the scope of our discussion here.

12 Continuum mechanics III: active complex fluids

We have conservation laws for mass and linear momentum. In both cases, we showed that the conservation law is of the same form. The time rate of change of a quantity is given by the divergence of a flux, plus some generation term for nonconserved quantities. When written in the comoving frame (that is, using the material derivative), we can define the flux tensor we need to specify. For conservation of linear momentum, this flux tensor is the stress tensor. The specification of the stress tensor is called a constitutive relation, and we have reasoned our way to them thus far (really, without proof). Now, we will move on to active fluids, which are a central topic in the papers we will read and discuss on the polarization of the *C. elegans* zygote.

12.1 Isotropic active viscous fluid

Our immediate goal is to model the acto-myosin cortex of the developing *C. elegans* embryo. The cortex is an example of an **active fluid**, in that it can exert stresses upon itself. This is achieved through the activity of motor proteins that cross-link actin filaments. Working together, the motors serve to compress the actin meshwork. We therefore add an active stress to the stress tensor. We will define the magnitude of this active stress to be σ_a. In general, this can be a function of myosin motor concentration or the concentration of any other factor that regulates actin or motor activity. We stipulate however that it is not a function of fluid velocity. So, the active stress in an isotropic fluid is a scalar quantity depending only on other scalar quantities. It therefore appears in the stress tensor must like the pressure, as $\sigma_a \delta_{ij}$. In this section, we will show that such a fluid cannot have any interesting dynamics beyond a passive fluid to motivate the need for the broken symmetry of a nematic active fluid.

Augmenting the stress tensor with the active stress, we have

$$\sigma_{ij} = -p\,\delta_{ij} + 2\eta\, v_{ij} + \sigma_a\, \delta_{ij}. \tag{12.1}$$

As a reminder, $v_{ij} = (\partial_i v_j + \partial_j v_i)/2$ is the symmetric part of the velocity gradient tensor. Apparently, from the definition of the stress tensor, the active stress is indistinguishable from the hydrostatic pressure, since they always appear together as a sum. Let us investigate this further by writing the equation of motion with the new stress tensor (again, assuming the dynamics are intertialess).

$$\eta\,\partial_j\partial_j v_i - \partial_i(p - \sigma_a) = 0. \tag{12.2}$$

As a step in exposing the active stress independence of the dynamics, we take the curl of both sides of the equation.

$$\varepsilon_{kli}\partial_k\left(\eta\,\partial_j\partial_j v_i - \partial_i(p - \sigma_a)\right) = \eta\,\partial_j\partial_j\,\omega_i = 0, \tag{12.3}$$

where we have defined the curl of the velocity field as the **vorticity**, ω_i (not to be confused the the antisymmetric part of the velocity gradient tensor, ω_{ij}). This tells us that the dynamics of the vorticity are given by

$$\partial_j \partial_j \omega_i = 0, \tag{12.4}$$

meaning that the motion is entirely determined by the boundary conditions.

Now, we will take the divergence of both sides of the equation of motion.

$$\partial_i \left(\eta \partial_j \partial_j v_i - \partial_i (p - \sigma_a) \right) = \eta \partial_j \partial_j [\partial_i v_i] - \partial_i \partial_i (p - \sigma_a) = 0. \tag{12.5}$$

The bracketed term is zero for an incompressible fluid by the continuity equation. Thus, the difference between the pressure and active stress are set by

$$\partial_i \partial_i (p - \sigma_a) = 0. \tag{12.6}$$

This equation must hold regardless of what the velocity field is to enforce incompressibility. Therefore, the quantity $p - \sigma_a$ is set entirely by incomressibility and the active stress can have no effect on the fluid dynamics that is distinguishable from the hydrostatic pressure. So, we cannot really model the cortex as an active incompressible isotropic fluid because this is indistinguishable from a non-active fluid.

12.2 Active nematic viscous fluid

The cortex consists of crosslinked filaments of actin. It therefore stands to reason that it is *not* isotropic because it consists of these stick like structures. We can define a local vector, called a **director** that describes the average orientation of the filaments in a small volume element. We will call this vector n_i and specify that it is a unit vector ($n_i n_i = 1$). We could define the local order in terms of n_i itself, but instead we will consider the case where the *sign* of the direction of the director is immaterial. Physically, this means that the "sticks" in the fluid do not have arrowheads; pointing in the positive x direction is the same as pointing in the negative x direction. In this case, we need to construct a **nematic order parameter** that respects this nondirectionality. As shown by de Gennes in the study of liquid crystals, this order parameter is a rank 2 tensor that can be constructed from the director as

$$Q_{ij} = S \left(n_i n_j - \frac{1}{3} \delta_{ij} \right). \tag{12.7}$$

Here, S is the magnitude of the local order. The nematic order parameter is symmetric and traceless.

Now that we have this order parameter that describes the fluid, we no longer have the isotropy we enjoyed when writing down the stress tensor for a simple fluid. We need to add an extra term to the stress tensor that takes into account nematic order.

$$\sigma_{ij} = -p \delta_{ij} + 2 \eta v_{ij} + \sigma_{ij}^{\text{nematic}}. \tag{12.8}$$

We will assume that we are above a critical temperature such that the filaments tend to be disordered. In other words, in a relaxed, equilibrium state, the order parameter tends toward zero. We might then write the nematic stress as a Taylor series about the $Q_{ij} = 0$ state, noting that the first order term should vanish because the nematic stress is minimal with $Q_{ij} = 0$.

$$\sigma_{ij}^{\text{nematic}} = A_{ijkl}Q_{kl} + B_{ijklmn}\partial_k\partial_l Q_{mn}. \tag{12.9}$$

From symmetry arguments and other approximations we will not go into here, the higher order tensors in the expansion can be reduced to scalars. As is traditionally done, we can define constants β_1, χ, and L and write the passive nematic stress as

$$\sigma_{ij}^{\text{nematic}} = \beta_1(\chi - L\partial_k\partial_k)Q_{ij}. \tag{12.10}$$

Here, χ is referred to as an inverse susceptibility and L is related to the Frank elastic constants from the theory of liquid crystals. The coefficient β_1 is an Onsager coefficient. We will not go into the details of these terms here (and this hand-wavy Taylor series expansion is not a careful derivation at all), but we write it this way because this is how it appears in the literature. So, the stress tensor for a passive nematic viscous fluid is

$$\sigma_{ij} = -p\,\delta_{ij} + 2\eta\, v_{ij} + \beta_1(\chi - L\partial_k\partial_k)Q_{ij}. \tag{12.11}$$

Next, we will write the active stress in terms of the order parameter. We can write it to linear order as a Taylor expansion.

$$\sigma_{\text{active}} = \sigma_a^0\,\delta_{ij} + \sigma_a Q_{ij}. \tag{12.12}$$

The first term describes the isotropic contraction due to active stresses. This is the same term as in the isotropic case and is indistinguishable from the pressure. We will therefore absorb it into the pressure and define $\Pi = p - \sigma_a^0$. The last term is directional stress exerted along the nematic order. So, our stress tensor for an active nematic fluid is

$$\sigma_{ij} = -\Pi\,\delta_{ij} + 2\eta\, v_{ij} + \beta_1(\chi - L\partial_k\partial_k)Q_{ij} + \sigma_a Q_{ij}. \tag{12.13}$$

The equation of motion is then, considering again the interialess limit for an incompressible fluid,

$$\partial_j\sigma_{ij} = 0 = -\partial_i\Pi + \eta\,\partial_j\partial_j v_i + \beta_1(\chi - L\partial_k\partial_k)\partial_j Q_{ij} + \partial_j(\sigma_a Q_{ij}). \tag{12.14}$$

12.3 Two-and-one-dimemsional active nematic fluid

In the homework, you will derive the equation of motion for an active nematic fluid that is confined to two dimensions. You will then make some assumptions about the

symmetry of the flow to reduce the result to a one-dimensional equation. This is the equation used in the Mayer, et al. and the Gross, et al. papers to describe the cortex dynamics. Specifically, you will derive that

$$-\eta\,\partial_x^2 v_x + \gamma\, v_x = \partial_x \sigma_a, \tag{12.15}$$

where γ is a friction coefficient. This equation means that gradients in active stress drive cortical flow against viscous dissipation and frictional losses.

Note that Q_{ij} does not appear in this equation. Nonetheless, to derive the equation of motion for the cortex, we do need to explicitly take into account nematic order.

13 Viscoelasticity and laser ablation

13.1 Linear viscoelasticity

We have so far considered the constitutive relations for an elastic solid and a viscous fluid (including active nematic viscous fluids). The actomyosin cortex behaves both elastically and viscously. For long time scales, it can flow, like a fluid. But if the cortex is rapidly stressed, it behaves like an elastic solid. After all, it is what gives the cell its shape. Further, as described in the Mayer, et al., paper, the actomyosin cortex responds elastically when it is cut while under tension. So, it has both elastic and viscous properties. What kind of constitutive relation describes this scenario of a **viscoelastic material**?

In many cases, it is not possible to write down a constitutive relation for a viscoelastic material. Researchers instead rely on experimental characterization of the material, such as a cell and its cortex, as it experiences stress.

Nonetheless, we can write down a linear theory that will (hopefully) provide some insight and predictive power. Let us compare for a moment the constitutive relations of an elastic and a viscous active nematic material. For simplicity, we will assume an incompressible material with a Poisson ratio of zero. For convenience, we will use the **shear modulus**, μ, which you can recall from equation (10.17) is the second Lamé coefficient. It is related to the Young's modulus by $\mu = E/2(1+\nu)$. In the case of zero Poisson ratio, this is $\mu = E/2$.

$$\text{elastic: } \sigma_{ij} + \Pi\,\delta_{ij} - \beta_1(\chi - L\partial_k\partial_k)Q_{ij} - \sigma_a Q_{ij} = 2\mu\,\varepsilon_{ij}, \tag{13.1}$$

$$\text{viscous: } \sigma_{ij} + \Pi\,\delta_{ij} - \beta_1(\chi - L\partial_k\partial_k)Q_{ij} - \sigma_a Q_{ij} = 2\eta\, v_{ij}. \tag{13.2}$$

Recall that

$$\partial_t \varepsilon_{ij} = \frac{1}{2}\,\partial_t(\partial_i u_j + \partial_j u_i) = \frac{1}{2}(\partial_i\partial_t u_j + \partial_j\partial_t u_i) = \frac{1}{2}(\partial_i v_j + \partial_j v_i) = v_{ij}. \tag{13.3}$$

So, if we differentiate the constitutive relation for the elastic material with respect to time, we get

$$\partial_t\,(\sigma_{ij} + \Pi\,\delta_{ij} - \beta_1(\chi - L\partial_k\partial_k)Q_{ij} - \sigma_a Q_{ij}) = 2\mu\, v_{ij}, \tag{13.4}$$

which we can re-write to give

$$\tau_{\mathrm{M}}\partial_t\,(\sigma_{ij} + \Pi\,\delta_{ij} - \beta_1(\chi - L\partial_k\partial_k)Q_{ij} - \sigma_a Q_{ij}) = 2\eta\, v_{ij}. \tag{13.5}$$

Here, $\tau_M = \eta/\mu$ is the **Maxwell time**, which describes the time scale for relaxation of elastic stresses. We might, then interpolate between the two cases of elastic and viscous materials by adding the constitutive relations together.

$$(1 + \tau_M\partial_t)\,[\sigma_{ij} + \Pi\,\delta_{ij} - \beta_1(\chi - L\partial_k\partial_k)Q_{ij} - \sigma_a Q_{ij}] = 2\eta\, v_{ij}. \tag{13.6}$$

For time scales much less than τ_M, the material behaves elastically, but for time scales much longer than τ_M, the material behaves viscously. This can be seen if we nondimensionalize time by the time scale of interest, τ. Then, the dimensionless operator at the front of equation (13.6) is

$$1 + \frac{\tau_M}{\tau}\,\partial_{\tilde{t}}. \tag{13.7}$$

If $\tau \gg \tau_M$, the second term is small and we get the constitutive relation for a viscous fluid. If $\tau \ll \tau_M$, the second term dominates, and we get the constitute relation for an elastic solid.

Equation (13.6) is actually not quite correct because it is not frame invariant. To see this, let's say that we did identical experiments on this viscoelastic material, one in a laboratory, and one in a train car moving at constant velocity v_i^0. Writing the stress tensor explicitly as a function of position and time, we have, for the time derivative of the stress tensor in the second experiment using the chain rule,

$$\partial_t \sigma_{ij}(x_i + v_k^0 t, t) = \partial_t \sigma_{ij} + v_k^0 \partial_k \sigma_{ij}. \tag{13.8}$$

Since the equation in this experiment has terms not present in the experiment done in the stationary lab, the governing equations are not frame invariant, which violates Gallilean relativity. Instead, we should use the **convected corotational derivative**, which preserves frame invariance, both for linear and rotational motion. The convected corotational derivative of a second rank tensor is defined as

$$\frac{\mathrm{D}A_{ij}}{\mathrm{D}t} = \partial_t A_{ij} + v_k \partial_k A_{ij} + \omega_{ik} A_{kj} + \omega_{jk} A_{ki}. \tag{13.9}$$

As a reminder, $\omega_{ij} = (\partial_i v_j - \partial_j v_i)/2$ is the antisymmetric part of the velocity gradient tensor. The convected corotational derivative is like the material derivative in that it sets the frame as the co-moving, corotational frame. So, for an active nematic viscoelastic fluid, which is solid-like at short time scales and viscous-like at long time scales, a linear viscoelastic model gives a constitutive relation of

$$\left(1 + \tau_M \frac{D}{Dt}\right)[\sigma_{ij} + \Pi\,\delta_{ij} - \beta_1(\chi - L\partial_k\partial_k)Q_{ij} - \sigma_a Q_{ij}] = 2\eta\, v_{ij}. \tag{13.10}$$

We will make use of this in interpreting the laser ablation experiments in the Mayer, et al. paper.

13.2 Analysis of cortical laser ablation experiments

In the Mayer, et al. paper, the authors used cortical laser ablation (COLA) to cut a line in the cortex of the *C. elegans* embryo and observe the recoil. By comparing

the initial velocity of the recoil of two different experiments, they could compare the total tension present in the cortex immediately before ablation. Why is this the case?

To address this question, we consider the cortex as an active nematic *elastic* material. In the elastic limit, we use the constitutive relation (13.1),

$$\sigma_{ij} = -\Pi\,\delta_{ij} + \beta_1(\chi - L\partial_k\partial_k)Q_{ij} + \sigma_a Q_{ij} + 2\mu\,\varepsilon_{ij}. \tag{13.11}$$

We assume that the nematic order is constant in space, so $\partial_k\partial_k Q_{ij} = 0$.

We assume the ablation line is along the y-direction so that the response is primarily along the x-direction. It is convenient, then, to write the xx-component of the constitutive relation.

$$\sigma_{xx} = -\Pi + (\beta_1\chi + \sigma_a)Q_{xx} + 2\mu\,\varepsilon_{xx}. \tag{13.12}$$

Note that in assuming the Poisson ratio is zero, motions in the y and z directions do not enter into the dynamics. If we had a nonzero Poisson ratio, we could still neglect these dynamics since $\varepsilon_{yy},\,\varepsilon_{zz} \ll \varepsilon_{xx}$ because the recoil is primarily in the x-direction.

Now we consider the geometry. The ablation line is at position $x = 0$. We define by x_c to be the position of the edge of the cortex at the ablation line. This moves as the cortex recoils from the ablation. For the purposes of this discussion, we will observe the right side of the ablation site. Now, $\varepsilon_{xx} = \partial_x u_x$, where u_x is the x-component of the displacement of the elements of the cortex from their equilibrium positions. If the deformation is distributed uniformly across the contracting cortex, the strain is $\varepsilon_{xx} = \partial_x u_x \approx (x_c - x_0)/(\ell - x_c)$. Here, the numerator is the displacement of the cortex from its equilibrium position x_0, and the denominator is the total length of the cortex. We have introduced ℓ as the total extent of the embryo. Prior to ablation, $x_c = 0$, so the initial strain is $\varepsilon^0_{xx} = -x_0/\ell$. For the stress, we have

$$\sigma_{xx} = -\Pi + (\beta_1\chi + \sigma_a)Q_{xx} + \frac{2\mu}{\ell - x_c}(x_c - x_0). \tag{13.13}$$

As the cortex initial retracts from the ablation, $\ell \gg x_c$, so the stress can be approximated as

$$\sigma_{xx} = -\Pi + (\beta_1\chi + \sigma_a)Q_{xx} + \frac{2\mu}{\ell}(x_c - x_0) = kx_c + \sigma^0_{xx}, \tag{13.14}$$

where we have defined a spring constant

$$k = 2\mu/\ell \tag{13.15}$$

and

$$\sigma^0_{xx} = -\Pi + (\beta_1\chi + \sigma_a)Q_{xx} - 2\mu\varepsilon^0_{xx} \tag{13.16}$$

as the stress present in the cortex immediately prior to ablation. Already we see that the active stress is not distinguishable in the dynamics, so we will not be able to ascertain it in an ablation experiment.

The cortex does not instantaneously achieve its new equilibrium. This is because there is dissipation due to friction with the surrounding membrane and cytoplasm. The above equation constitutes a force balance, and we need to also include the frictional force. This will be proportional to the velocity of the recoil, or $\partial_t x_c$. Thus, we get

$$\sigma_{xx} = kx_c + \sigma_{xx}^0 + \zeta \partial_t x_c, \tag{13.17}$$

where ζ is the friction coefficient. With this force balance, we can study the dynamics of the recoil from a COLA experiment. Upon ablation, the cortex can no longer support stresses because the material has been destroyed, so $\sigma_{xx} = 0$. Thus, we take $\sigma_{xx}(t) = \sigma_{xx}^0(1 - \theta(t))$, where $\theta(t)$ is a unit step function. Then, we are left with the ODE

$$\zeta \partial_t x_c = -kx_c - \sigma_{xx}^0 + \sigma_{xx}^0(1 - \theta(t)) = -kx_c - \sigma_{xx}^0 \theta(t). \tag{13.18}$$

If the ablation happens at time $t = 0$, then for $t < 0$, we have $\partial_t x_c = 0$, since $x_c(t = 0) = 0$. For $t > 0$, we have

$$\zeta \partial_t x_c = -kx_c - \sigma_{xx}^0. \tag{13.19}$$

This first order linear differential equation is solved to give

$$x_c(t) = c\, \mathrm{e}^{-kt/\zeta} - \frac{\sigma_{xx}^0}{k} \tag{13.20}$$

where c is a constant of integration. We match to the initial condition that $x_c = 0$ to get that $c = \sigma_{xx}^0/k$. Thus, we have

$$x_c(t) = \frac{\sigma_{xx}^0}{k}(1 - \mathrm{e}^{-kt/\zeta}). \tag{13.21}$$

The outward velocity of the bleeding edge of the ablation is then

$$v(t) = \partial_t x_c = \frac{\sigma_{xx}^0}{\zeta}\, \mathrm{e}^{-kt/\zeta}. \tag{13.22}$$

So, the initial outward velocity is σ_{xx}^0/ζ, which is proportional to the total x-directional stress that was present in the cortex immediately prior to ablation. We cannot assess the value of σ_{xx}^0 because we do not know what ζ is. And, as mentioned before, we also cannot tell how much of the total stress is due to active stress. However, we can compare experiments to see the *relative* magnitudes of the total stress present in the cortex. Further, if ζ is the same across experiments, which we would expect it to be, the decay of the outward velocity is proportional to the stiffness (the Young's modulus) of the cortex. We note, though, that this result is only valid for times shortly after the ablation, because the cortex is viscoelastic, so it loses its elastic character at longer times. Furthermore, the *C. elegans* cortex has a wound-healing response at longer times as well.